The Pacific decadal oscillation, revisited

Matthew Newman[1,2*], Michael A. Alexander[2], Toby R. Ault[3], Kim M. Cobb[4], Clara Deser[5], Emanuele Di Lorenzo[4], Nathan J. Mantua[6], Arthur J. Miller[7], Shoshiro Minobe[8], Hisashi Nakamura[9], Niklas Schneider[10], Daniel J. Vimont[11], Adam S. Phillips[5], James D. Scott[1,2], and Catherine A. Smith[1,2]

[1]CIRES, University of Colorado, Boulder, Colorado
[2]NOAA Earth Systems Research Laboratory, Boulder, Colorado
[3]Department of Earth and Atmospheric Sciences, Cornell University, Ithaca, New York
[4]School of Earth and Atmospheric Sciences, Georgia Tech, Atlanta, Georgia
[5]Climate and Global Dynamics, National Center for Atmospheric Research, Boulder, Colorado
[6]NOAA Southwest Fisheries Science Center, Santa Cruz, California
[7]Scripps Institute of Oceanography, La Jolla, California
[8]Graduate School of Science, Hokkaido University, Sapporo, Japan
[9]Research Center for Advanced Science and Technology, The University of Tokyo, Tokyo, and Research Institute for Global Change, JAMSTEC, Yokohama, Japan
[10]Department of Oceanography and International Pacific Research Center, University of Hawai`i at Manoa, Honolulu, Hawaii
[11]Department Of Atmospheric and Oceanic Sciences, and Nelson Institute Center for Climatic Research, University of Wisconsin-Madison, Madison, Wisconsin

Submitted to *Bull. Amer. Meteor. Soc.*, March 3 2015

[*] *Corresponding author address:* Matthew Newman, NOAA/ESRL, 325 Broadway, R/PSD1, Boulder, CO 80305.
E-mail: matt.newman@noaa.gov

Abstract

The Pacific decadal oscillation (PDO) is the target of ongoing research within the meteorological and climate dynamics communities, and is central to the work of many geologists, ecologists, natural resource managers, and social scientists. Research over the last decade has led to an emerging consensus regarding the physical processes that drive the PDO, including both remote tropical forcing and local atmosphere/ocean processes. PDO-related regional impacts should account for the effects of these different processes, which operate on different timescales and only partly represent direct forcing of the atmosphere by the North Pacific Ocean.

Capsule

Different physical processes combine to drive variability of the PDO, which carries implications for its use in climate impact studies, forecasts, and projections.

Introduction

Since its identification in the late 1990's as the dominant year-round pattern of North Pacific sea surface temperature (SST) variability, the Pacific decadal oscillation (PDO) has been connected both to other parts of the climate system and to impacts on natural resources and marine and terrestrial ecosystems. Subsequent research, however, has found that the PDO is not a single physical mode of climate variability but instead largely represents the combination of three groups of processes: (1) changes in ocean surface heat fluxes and Ekman (wind-driven) transport related to the Aleutian low, due to both local unpredictable weather "noise" and to remote forcing from interannual to decadal tropical variability (largely El Niño) via the "atmospheric bridge"; (2) ocean memory, or processes determining oceanic thermal inertia including "re-emergence", that act to integrate this forcing and thus generate added PDO variability on interannual and decadal time scales; and (3) decadal changes in the Kuroshio-Oyashio current system, forced by winds over the North Pacific driving westward propagating oceanic Rossby waves, manifested as SST anomalies along the subarctic front at about 40ºN in the western Pacific ocean. Thus, the PDO represents the effects of different processes operating on different timescales, and its apparent impacts only partly represent direct forcing of the atmosphere by the North Pacific Ocean. This paper synthesizes this current view of the PDO and discusses its implications for climate diagnosis, including PDO climate impacts and predictability (both oceanographic and atmospheric); potential decadal "regime"-like

68 behavior; PDO simulations in climate models; the interpretation of multicentennial PDO
69 reconstructions; and its impacts on marine ecosystems. We conclude with a few
70 suggested "best practices" for future PDO-based diagnosis and forecasts.

71 **What is the PDO?**

72 The PDO was first introduced by Mantua et al. (1997) as the leading Empirical
73 Orthogonal Function (EOF) of North Pacific (20º-70ºN) SST monthly-averaged
74 anomalies, defined as departures from the climatological annual cycle after removing the
75 global mean SSTs. Figure 1a shows the PDO pattern, calculated by regressing SST
76 anomalies on the EOF's expansion coefficient time series (or Principal Component; PC),
77 obtained from the HadISST dataset (Rayner et al. 2003) for the years 1901-2004. [Unless
78 otherwise noted, this dataset and period are used for all calculations in this paper.] Over
79 this period, the PDO is fairly similar across SST datasets, which all use different methods
80 to "fill in" missing grids, with relatively minor differences both in time series (Fig. 1c)
81 and pattern (Fig. 1d, where each triangle represents the "distance" of the HadISST PDO
82 pattern from the PDO pattern of a different dataset). It is also reasonably robust to
83 sampling; for example, continually repeating the EOF analysis upon randomly chosen
84 (with replacement) 50-year draws from the HadISST dataset yields patterns all very
85 highly correlated with the PDO EOF (the black dots in Fig. 1d represent how the
86 resulting patterns of this "Monte Carlo" test differ from the full dataset PDO). Dataset
87 dependencies are more pronounced early in the observational record and when only a few
88 decades are used to define the climatology and leading EOF (Wen et al. 2014).

89 Two characteristics of the PDO found by researchers in the 1990's suggested it
90 might represent a distinct physical "mode" of North Pacific variability. First, even using

monthly anomalies, the PDO time series has a slowly varying component, with episodic changes of sign; hence "decadal oscillation"[1]. Second, there were reasons to view the PDO as a potentially independent North Pacific mode, since the PDO and the Tropics appeared only weakly coupled as evidenced by the low *simultaneous* correlation between time series of the PDO and eastern equatorial Pacific SST anomalies. Additionally, some early modeling work (Latif and Barnett 1994; 1996) raised the possibility that the PDO might correspond to a physical mode, oscillating on decadal time scales, of coupled atmosphere-ocean interaction within the North Pacific.

As the leading North Pacific EOF, the PDO is, *by construction*, the pattern whose variation best encapsulates variability of monthly SST anomalies (SSTAs) within the domain where it is defined (that is, the PDO "explains the most variance" in the North Pacific). However, the PDO does not have to be exclusive to the North Pacific, and in fact the observed regression pattern in Fig. 1a shows a strong connection between the North Pacific and the Tropics, except for the eastern equatorial cold tongue between 2ºN-2ºS (Deser et al. 2004). In particular, positive SSTAs in the eastern tropical Pacific accompany negative SSTAs in the central and western North Pacific and positive SSTAs in the eastern North Pacific (Fig. 1a). Also, some PDO details depend upon the domain used for the EOF calculation: as this domain is expanded southward (orange symbols in Fig. 1d), the tropical portion of the pattern becomes relatively more pronounced, even along the equator, with the North Pacific anomaly shifting slightly eastward to become more symmetric with its South Pacific counterpart. The leading SST EOF of the entire Pacific basin resembles a global ENSO-related pattern (e.g., Deser and Blackmon 1995).

[1] Note that in meteorological parlance, "oscillation" was first related to *spatial* sea-saw patterns in the Atlantic and Pacific by Walker and Bliss (1932), which has more recently been occasionally confused with *temporal* oscillations.

Moreover, the PDO bears considerable similarity to patterns of ENSO-like decadal variability (Zhang et al. 1997; Barlow et al. 2001; Deser et al. 2004), including the Interdecadal Pacific Oscillation (IPO; Power et al. 1999; Folland et al. 2002; Parker et al. 2007; Dai 2012), that are constructed by first filtering SSTAs to remove interannual variability. It is not identical, however: the monthly IPO time series (Folland 2008) has a 0.8 correlation with the PDO index, whereas the IPO has a 0.95 correlation with the time series of the leading Pacific basin EOF.

Processes driving the PDO

Statistical modes may represent physical modes, but there need not be a one-to-one correspondence between them. A body of research exists showing how different physical processes, including random atmospheric forcing; teleconnections from the tropical Pacific; and ocean Rossby waves/shifts in the basin-wide ocean gyre circulation, contribute to PDO variability on a variety of time scales and in different parts of the North Pacific Ocean.

FLUCTUATIONS IN THE ALEUTIAN LOW (LARGE-SCALE STOCHASTIC FORCING)

Many aspects of climate can be represented by a slow dynamical system integrating fast forcing approximated as random, or stochastic, noise (Hasselmann 1976). In a simple stochastic model of midlatitude SST variability (Frankignoul and Hasselmann 1977), the ocean at a given location is treated as a motionless (well-) mixed layer in which surface heat fluxes both force and damp SSTAs. The forcing F is represented by fluxes associated with weather variations, which relative to oceanic time scales have

approximately no memory and the same variance at all time scales ("white noise"). The resulting SSTAs are damped by a linear negative air-sea feedback, representing loss (gain) of heat with the atmosphere from anomalously warm (cold) waters. This can be expressed as a first order autoregressive or *AR1* model,

$$SST(n) = r\, SST(n\text{-}1) + F, \quad (1)$$

where r represents the expected fraction of the SSTA retained (i.e., not lost to damping) between times $n\text{-}1$ and n, determined by the feedback of air-sea heat fluxes and SST and by the thermal inertia of the upper ocean in direct contact with the atmosphere. Then the SSTAs exhibit a "red noise" spectrum whose magnitude increases with the inverse square of frequency, flattening out at periods long compared to the damping time scale.

The simple view of SST variability as a product of noise integration can be applied basin-wide. White noise forcing associated with large-scale weather generates much of the observed SST variability over the entire North Pacific Ocean (Frankignoul and Reynolds 1983), where interannual variability in the surface fluxes and SSTs are closely linked to dominant atmospheric circulation patterns (Cayan 1992; Iwasaka and Wallace 1995). In an atmospheric general circulation model (AGCM) coupled to a mixed layer ocean model with no currents (and hence no ENSO variability or ocean dynamics), the dominant sea level pressure (SLP) pattern is associated with fluctuations in the strength of the Aleutian low pressure system primarily resulting from internal atmospheric dynamics (Pierce 2001; Alexander 2010), including large-scale dominant teleconnection patterns such as the Pacific-North American (PNA) pattern. For periods with a stronger low, enhanced wind speeds and reduced air temperature and humidity along ~35°N cool the underlying ocean via surface sensible and latent heat fluxes, while

158 northward advection of warm moist air heats the ocean near North America (Fig. 1a); the
159 opposite flux anomalies occur when the low is weaker than average. The simulated flux-
160 driven SSTA pattern in the North Pacific closely resembles the observed PDO.
161 Anomalous Ekman transports tend to amplify the flux-driven pattern (Miller et al.
162 1994b). These physical processes result in observed correlations between the North
163 Pacific index (NPI), a measure of the Aleutian low, and SST that are high when the NPI
164 leads SST (Fig. 2a) but low when SST leads the NPI (Fig. 2b) (Davis 1976; Deser and
165 Timlin 1998); similar results are obtained using the PNA index (Fig. S3c).

166 TELECONNECTIONS FROM THE TROPICS

167 *a. Interannual timescales*

168 Noise due to intrinsic mid-latitude atmospheric variability is but one source of the
169 forcing F in (1). ENSO SSTAs in the tropical Pacific induce global atmospheric
170 teleconnections (e.g. see Trenberth et al. 1998; Liu and Alexander 2007) altering near-
171 surface air temperature, humidity, wind, and clouds far from the equatorial Pacific. The
172 resulting variations in the surface heat, momentum, and freshwater fluxes cause changes
173 in SST and ocean currents. Thus, during ENSO events an "atmospheric bridge" extends
174 from the equatorial Pacific to other ocean basins including the North Pacific (e.g.,
175 Alexander 1990, 1992; Lau and Nath 1994, 1996, 2001; Alexander et al. 2002). When El
176 Niño events peak in boreal winter, the Aleutian low deepens and the changes in the
177 surface heat fluxes, wind driven mixing, and Ekman transport in the upper ocean all act
178 to create a positive PDO SSTA pattern (Alexander et al. 2002, Alexander and Scott 2008;
179 see also Strong and Magnusdottir 2009). This relationship, easily seen by correlating a
180 wintertime ENSO index (here, the time series of the leading tropical SSTA EOF) with

subsequent global springtime SSTAs (Fig. 2c), is quite stable throughout the observational record, with some amplitude changes but little modification in pattern (see Fig. S4). A similar signal also exists in the South Pacific (e.g., Shakun and Shaman 2009; Deser et al. 2004), helping give rise to the more meridionally symmetric IPO pattern. In general, ENSO leads the PDO throughout the year (Newman et al. 2003), but the bridge acts differently in summer and fall, when it modifies SSTAs in the west Pacific primarily through changes in cloudiness (Alexander et al. 2004).

b. Decadal time scales

Zhang et al. (1997) employed several techniques to separate interannual and "interdecadal" (> 6 yr) ENSO variability. The SSTA pattern based on their low-pass filtered data, later identified as the IPO (Power et al. 1999; Parker et al. 2007), is similar to the unfiltered ENSO pattern except it is broader in scale in the eastern equatorial Pacific and has enhanced extratropical magnitude relative to the Tropics; its North Pacific component resembles the PDO. Other statistical methods of decomposing the data indicate that some portion of the decadal variability in the PDO region is associated with low frequency anomalies in the tropical Pacific (e.g. Nakamura et al., 1997; Mestas Nuñez and Enfield 1999; Seager et al. 2004; Deser et al. 2004; Vimont 2005; Alexander et al. 2008a). Based on experiments using an atmospheric GCM coupled to a global mixed layer ocean model except in the tropical Pacific, where observed SSTs were specified, Alexander et al. (2002) and Alexander (2010) estimated that ¼ - ½ of the PDO-related variability was associated with tropical Pacific decadal variability, communicated to the North Pacific via the atmospheric bridge.

MIDLATITUDE OCEAN DYNAMICS AND COUPLED VARIABILITY

a. Re-emergence

We might expect that, due to the thermal capacity of seawater and typical mixed layer depths, the memory time scale of the ocean is on the order of months. However, due to seasonal variations in the ocean mixed layer depth, the time scale of midlatitude SSTAs in successive cold seasons is generally greater than a year. Figure 2d illustrates this process, showing the correlation of FMA PDO values with central North Pacific ocean temperatures at depth and increasing lag. [Fig. S5 shows results for other regions.] Persistent temperature anomalies forming at the surface are mixed downwards throughout the deep winter mixed layer. Then, when the mixed layer abruptly shallows in spring, thermal anomalies at depth can remain under the summer seasonal thermocline, insulated from surface fluxes that damp anomalies in the thin mixed layer above. When the mixed layer deepens again in the following fall, the deeper anomalies are mixed back towards the sea surface. This process, first noted by Namias and Born (1970, 1974) and termed the "reemergence mechanism" by Alexander and Deser (1995), occurs over large portions of the North Atlantic and North Pacific Oceans (Alexander et al. 1999; 2001; Bhatt et al. 1998; Timlin et al. 2002; Hanawa and Sugimoto 2004). The PDO SSTA pattern, generated by internal atmospheric dynamics and/or the atmospheric bridge, recurs in consecutive winters via the reemergence mechanism (Alexander et al. 1999, 2001, 2002), while the summertime PDO signal (at the surface, at least; Fig. 2d) does not tend to recur (Nakamura and Yamagata 1999) and is instead largely forced by contemporaneous air-sea fluxes. Thus the reemergence mechanism determines the effective thermal inertia and the value of r in (1) as corresponding to deep winter mixed

layers (Deser et al. 2003), enhancing PDO variability on interannual to decadal time scales (Newman et al. 2003; Schneider and Cornuelle 2005).

b. Ocean gyre dynamics

Much of the dynamics within the North Pacific Ocean involves two basin-wide circulations of water, a subpolar counterclockwise gyre and subtropical clockwise gyre, separated by a sharp meridional SST gradient called the subarctic frontal zone (SAFZ). In the western Pacific, large SST variations associated with the PDO occur within the SAFZ, specifically in the Kuroshio Extension (KE) and Oyashio frontal zones and the mixed water region in between (Nakamura et al. 1997; Nakamura and Kazmin 2003; Nonaka et al. 2006). While in most of the North Pacific, SST variability is driven primarily by atmospheric forcing (Smirnov et al. 2014), in this region persistent warm (cool) SSTAs in winter tend to enhance (reduce) heat and moisture fluxes into the atmosphere (Tanimoto et al. 2003; Taguchi et al. 2012), a consequence of dynamic adjustment of upper-ocean gyre circulations that contributes to F in (1). The adjustment occurs primarily through westward propagating Rossby waves excited by anomalous wind stress curl (Miller et al. 1998; Deser et al. 1999; Seager et al. 2001; Schneider et al. 2002; Qiu and Chen 2005; Taguchi et al. 2007). These waves, whose sea surface height variations can be measured by satellite (Fig. 2f), take several (3-10) years to cross the basin guided by the KE jet (Sasaki and Schneider 2011, Sasaki et al. 2013), producing primarily decadal variability in F with a red spectra without preferred spectral peaks (Frankignoul et al. 1997). Specifically, SSTAs result (Fig. 2e) from shifts of latitude and intensity of the fronts (Qiu 2003; Nakamura and Kazmin 2003; Taguchi et al. 2007), and modulations of the stability of the KE jet, the recirculation gyre (Qiu 2000, 2002; Qiu and

249 Chen 2005, 2010; Kelly et al. 2010; Kwon et al. 2010) and thereby eddy-driven heat
250 transports (Sugimoto and Hanawa 2011). The latitude of the shallow Oyashio front, by
251 contrast, may be more sensitive to local wind forcing (Nonaka et al. 2006).
252 An atmospheric response to PDO SST variations could enhance PDO decadal
253 variance, or lead to a preferred time scale, if the response projects on F in (1) as a
254 positive or delayed negative, respectively, feedback on the PDO. A basic thermodynamic
255 response exists: the temperature difference between atmospheric boundary layer and
256 oceanic mixed layer decreases due to air-sea heat exchange, slowing subsequent heat
257 exchanges that depend upon this difference, producing "reduced thermal damping"
258 (Barsugli and Battisti 1998) with a consequent increase of temperature variability (Blade
259 1997). Stochastic wind forcing whose spatial scale corresponds to certain ocean advective
260 (transport) scales might also resonantly enhance decadal SST variability without other
261 feedbacks (Saravanan and McWilliams 1998).
262 The nature of the coupled ocean-atmosphere dynamical response to PDO SSTAs has
263 been less clear. Such dynamical feedbacks were once thought to drive oscillatory
264 behavior in the PDO (Latif and Barnett 1994), but almost all subsequent studies found
265 that the necessary atmospheric response was too weak, or even of the wrong sign, to
266 generate sustained oscillations. On the one hand, recent observational studies
267 (Frankignoul et al. 2011; Taguchi et al. 2012), coupled GCM experiments (Kwon and
268 Deser 2007; Taguchi et al. 2012) and observationally derived heuristic models (Qiu et al.
269 2007) suggest that the atmospheric response to SSTAs in the KE and Oyashio frontal
270 zones could induce a modest atmospheric response in the anomalous Aleutian low, which
271 may be able to enhance variability at decadal periods. Those SST frontal zones may act to

anchor the Pacific storm track (Nakamura et al. 2004), and its feedback forcing seems important in maintaining a stationary atmospheric response (Taguchi et al. 2012; Okajima et al. 2014). On the other hand, AGCM studies have yet to agree on even the sign of the atmospheric response to warm SSTAs in the frontal zones, with sensitivity to many factors including the simulated direct response to the low-level heating, downstream eddy feedbacks of the modulated storm track, and dependencies upon seasonality and base state (Okajima et al. 2014; see also review by Kushnir et al. 2002). Likewise, wind forcing of the ocean driven by the atmospheric response to frontal zone SSTAs found by Kwon and Deser (2007) was of one sign across the Pacific at ~40°N, while Qiu et al. (2007) found that its counterpart to the KE variability switched signs in the center of the basin. Also, Frankignoul et al. (2011) and Taguchi et al. (2012) observed an anomalous surface Aleutian Low in response to KE/Oyashio fronts SSTAs that, however, was accompanied by different upper-level anomalies. Some recent observational analysis, and model experiments at finer resolution (typically ~25 km), suggests that a robust atmospheric response to KOE SSTAs may instead involve significant changes in poleward heat and moisture transports by individual storms (O'Reilly and Czaja 2015) that may not be captured by currently typical climate model resolution (Smirnov et al. 2015), so the impact of ocean-atmosphere coupling onto the PDO is still not fully understood.

c. Summertime air-sea feedbacks

During summer, due to both a shallower seasonal thermocline and weaker atmospheric variability, the PDO tends to be less persistent and less confined to the oceanic frontal zones (Nakamura and Kazmin 2003). Instead, SST variability may be

linked to anomalous low-level cloudiness. Over the NE Pacific, for example, where summertime mid-tropospheric subsidence is maintained by the climatological subtropical high (Miyasaka and Nakamura 2005), most of the clouds develop under the capped inversion layer (Klein et al. 1995: Norris 1998; Wood 2012). Decadal enhancement of lower-tropospheric static stability, due both to negative SSTAs and stronger subsidence associated with the intensified subtropical high, acts to increase low-level cloud amount, optical depth and planetary albedo, and vice versa (cf. Clement et al. 2009). The resulting anomalous cloud radiative forcing could enhance the underlying SSTA as positive feedback. Over the NW Pacific, low-level cloudiness is climatologically high in summer, but is less variable than over the NE Pacific (Norris et al. 1998), which is particularly the case over the subpolar oceanic gyre. Still, decadal variability in low-level cloudiness tends to maximize around 35°N to the south of the NP SAFZ.

The PDO as the sum of multiple processes

In this section we employ two approaches, empirical and numerical modeling studies, to explore how PDO processes combine to produce PDO variability.

EMPIRICAL ANALYSIS

Several recent studies extended the simple AR1 model (1) to incorporate additional PDO dynamical processes discussed above. Using annually-averaged (July-June) anomalies, Newman et al. (2003) found that (1) could be improved by including ENSO forcing within F, with the revised empirical AR-1 model now

$$PDO(n) = r\, PDO(n-1) + a\, ENSO(n) + noise\ . \qquad (2)$$

316 Note that *r*, corresponding to a time scale of ~2 years, includes reemergence, amplifying
317 the low-frequency ENSO component of PDO variability (producing a "reddened
318 ENSO"). Schneider and Cornuelle (2005) included shifts in the North Pacific Ocean
319 gyres in *F* and explicitly represented anomalous Aleutian low forcing, finding that on
320 interannual time scales, random Aleutian Low fluctuations and ENSO teleconnections
321 were about equally important in determining PDO variability with negligible
322 contributions from ocean currents, while on decadal time scales stochastic forcing,
323 ENSO, and changes in the gyre circulations each contributed approximately 1/3 of the
324 PDO variance. The primary implication of these analyses is that, unlike ENSO, the PDO
325 is likely not a single physical mode but rather the sum of several different basin-scale
326 processes (eg; Schneider and Cornuelle 2005; Newman 2007, 2013; Alexander et al.
327 2008b).

328 An interesting feature of these processes is that while their patterns are not
329 identical (for example, compare Figs. 2a and 2c) and their characteristic time scales are
330 quite different, they all project strongly onto the PDO pattern. However, many common
331 analysis techniques, such as the EOF/PC calculation presented earlier, cannot distinguish
332 between spatially similar, or nonorthogonal, patterns with differing evolution. One
333 method that can involves extending the AR1 model from one to many variables, such as
334 SSTAs throughout the tropical and North Pacific oceans. The resulting multivariate AR1
335 model (Linear Inverse Model (LIM); Penland and Sardeshmukh 1995; Newman 2007;
336 Alexander et al. 2008b) yields patterns, or eigenmodes, that also represent different
337 dynamical processes with different evolution, but potentially similar spatial structure.
338 Each has its own time scale (its own value of *r*, in analogy with (1)), but not all the

patterns are static (some also evolve with characteristic frequency). Here we extend the LIM of Newman (2007) to higher spatial and temporal resolution (a full description of the approach can be found there); as in that study and related analyses (Compo and Sardeshmukh 2010; Newman 2013), the pattern corresponding to the global mean temperature time series makes almost no contribution to the PDO.

Ordered by decreasing memory time scale, the three eigenmodes in Fig. 3 represent dynamical processes with maxima in the North, central tropical/northern subtropical, and eastern tropical Pacific, respectively; similar patterns have been reported elsewhere (eg, Barlow et al. 2001; Chiang and Vimont 2004; Guan and Nigam 2008; Compo and Sardeshmukh 2010). Each eigenmode's contribution to the PDO time series (also in Fig. 3) when summed yields a reconstructed PDO (Fig. 3g) quite similar to the full PDO (Fig. 3h), with 0.7 correlation that increases to 0.8 when both are smoothed with the 6-yr lowpass filter used in Fig. 1c. The residual between the two time series is mostly noise since its memory time scale is ~5 months.

One oft-noted PDO aspect, both in climate (e.g., Ebbesmeyer et al. 1991; Graham 1994; Mantua et al. 1997; Minobe 1997; Fleming 2009; Minobe 2012) and ecological (e.g., Yasuda et al. 1997; Hare and Mantua 2000; Chavez et al. 2003; Peterson and Schwing 2003) studies, is the appearance of "regime shifts" every few decades or so. The green lines in Figs. 3g-h indicate that such times for the PDO are also captured by the reconstructed PDO. Such occurrences (if significant; Rudnick and Davis 2003) might represent sudden nonlinear changes between relatively stable climate states. However, regime shifts are also well known to exist in aggregations of AR1 processes (Granger 1980; Beran 1994). To the extent that the PDO represents an aggregation of several

362 basin-scale dynamical processes with differing but substantial projection onto the PDO
363 pattern, each PDO regime could represent different combinations of processes (see also
364 Deser et al. 2004), with regime shifts due to randomly forced variations in the
365 superposition of these processes (Newman 2007).

366 In other words, PDO climate regime shifts could be an artifact of measuring the
367 multivariate North Pacific Ocean climate system with a single index (eg, the PDO). This
368 is illustrated by comparing multidecadal global SST change across the 1976/77 regime
369 shift to corresponding change across 1969/70, chosen since the most slowly varying PDO
370 component changed sign then (Fig. 3a). For the 1976/77 regime shift (Fig. 3j), the well-
371 documented warming in the Tropical IndoPacific and along the west coast of North
372 America is evident, along with central Northeast Pacific cooling (e.g., Graham 1994;
373 Miller et al. 1994a; Meehl et al. 2009), whereas 1969/70 (Fig. 3i) marked a North Pacific
374 cooling with greater amplitude that, not surprisingly, extended further westward; note
375 also a corresponding signal in the Atlantic. Which year was "the" regime shift in the
376 North Pacific?

377 PDO REPRESENTATION BY COUPLED CLIMATE MODELS

378 Perhaps our most comprehensive tool for understanding how processes interact to
379 produce the PDO is the coupled general circulation model (CGCM). Here, we assess
380 CGCM reproduction of the PDO and PDO processes.

381 Figure 1b exemplifies the range of PDO patterns (defined according to Mantua et
382 al. 1997) across the "historical" CMIP5 models, used in the most recent IPCC assessment
383 to evaluate impacts of observed radiative forcing, in comparison with the observed
384 pattern (Fig. 1a). The complete range of CMIP5 PDO patterns is in Fig. S1, with

associated time series in Fig. S2 (Phillips et al. 2014). Some models faithfully depict the observed spatial pattern ("Model A") while others lack the tropical connection ("Model B"). The Taylor diagram in Fig. 1d quantifies how well each modeled PDO matches observations; the distance of each symbol from the reference (observations) represents the rms error of each model PDO pattern. While in each case, the North Pacific SSTA pattern resembles observations and is accompanied by a realistic SLP anomaly (see also Sheffield et al. 2013; Yim et al. 2014), virtually none of the simulations are within the range of either dataset or sampling uncertainty. The spatial relationship between North Pacific SST and SLP anomalies reflects observations, with the atmosphere forcing the ocean and not vice versa, although the model PDO response to atmospheric forcing tends to persist longer than observed (Fig. S3c).

Due to the chaotic nature of the climate system, even very small differences in initial conditions cause simulations to diverge from nature. Hence, in the absence of an externally forced signal, we expect CGCMs to represent PDO variability statistics but not the observed PDO time series. Fig. 1c shows that the CMIP5 historical PDO time series (here smoothed with the 6-yr lowpass filter) are, as expected, all quite different; in particular, none reproduce the observed 20th century sequence of PDO "regimes". Additionally, the ensemble mean of all the time series is near-zero. Given that these model runs are forced with the post-1850 history of radiative forcing, Fig. 1c suggests that the externally forced PDO signal is negligible, consistent with the above empirical analysis, and that the PDO represents natural internal variability.

Earlier analysis of CMIP3 models showed that almost all underestimated the ENSO-PDO relationship compared to observations (Newman 2007; Oshima and

Tanimoto 2009; Furtado et al. 2011; Lienert et al. 2011; Deser et al. 2012; Park et al. 2013). To investigate how the representation of tropical-extratropical interaction impacts the PDO in the CMIP5 historical runs, we fit each PDO time series with the AR-1 model

$$\mathrm{PDO}(n)=r\,\mathrm{PDO}(n\text{-}1) + a\,\mathrm{ENSO1}(n) + b\,\mathrm{ENSO2}(n) + \varepsilon(n), \quad (3)$$

where PDO is the PDO time series, ENSO1 and ENSO2 are the time coefficients of the leading two EOFs of tropical Pacific (20°S–20°N) SSTAs, ε is white noise, and n is time step. The AR-1 model, estimated for detrended and normalized annual mean time series averaged from July to June, follows the approach introduced in (2) but includes potential diversity in ENSO anomalies (e.g., Capotondi et al. 2015) with ENSO2; note that ENSO1 is essentially the same as the ENSO index used above.

The AR-1 models constructed from observations and the CMIP5 runs have several notable differences. First, tropical forcing of the PDO is dominated by ENSO1 (Fig. 4b) in observations, but not for most CMIP5 runs. Also, the AR-1 model performance ρ, evaluated by correlating each PDO time series with its corresponding AR-1 model estimate, is higher for observations than for most CMIP5 runs (Fig. 4d); this performance is related to the ENSO1 forcing coefficient, with ρ and a correlated at 0.7. On the other hand, forcing by ENSO2 (Fig. 4c) for all the CMIP5 models is generally greater than for observations. These differences in the relative magnitudes of a and b indicate that the tropics-to-PDO linkage is different both quantitatively and qualitatively between most CMIP5 models and observations (see also Fig. S3b). Also, note that most CMIP5 models have larger values of r as well as longer overall autocorrelation times than observed (Fig. S3a), suggesting that mechanisms causing persistence of the PDO such as oceanic vertical mixing, SST reemergence, oceanic Rossby wave propagation, and/or

ocean-to-atmosphere feedback in mid-latitudes play a stronger role in CMIP5 models than in observations (also, there is less noise in the model output than in observations). Why this is remains to be understood.

Decadal to centennial PDO variability

As with simpler AR1 models, the LIM generates confidence intervals for power spectra. Figure 5 shows that PDO spectra calculated from observations and the CMIP5 simulations (both control and historical) all generally lie within these confidence intervals. So too do the 1000-yr, externally forced "last millennium" CMIP5 simulations that include estimates of explosive volcanism, solar variability, and anthropogenic changes to atmospheric composition and land use since 850, again suggesting that the PDO largely represents internal, unforced variability, even on decadal to centennial (or dec-cen) timescales. However, given that the CMIP5 PDO connections to the Tropics are generally too weak, and that unforced CMIP5 models generally underestimate dec-cen tropical SST variability (Ault et al. 2013; Laepple and Huybers 2014), the agreement between the CMIP5 power spectra and the LIM may be somewhat fortuitous. That is, some of the "reddened ENSO" power in observations is missing in the models, but its loss seems compensated by an overestimate of the persistence of internally-generated North Pacific SSTAs.

Even relative to a univariate AR1 (red noise) process, no statistically significant decadal or multidecadal peaks in these spectra are detectable (Pierce 2001). Rather, PDO spectral power appears to continually increase with decreasing frequency f, raising the possibility that the spectra represent not red noise but rather long-memory, "1/f noise" (Keshner 1982), with potentially pronounced regime behavior (eg, Percival et al. 2001;

454 Overland et al. 2006; Fleming 2014; see also Fraedrich et al. 2004). However, the LIM
455 spectrum also is not flat over multidecadal time scales. In fact, spectral slopes are a
456 characteristic not only of some nonlinear systems but also aggregation of processes
457 resulting from a multivariate AR1 system driven by noise (Milotti 1995; see also Penland
458 and Sardeshmukh 2012).

459 Spectra for several reconstructions of the PDO made by combining paleoclimate
460 proxies such as tree rings, corals, and sediments (Table 1), stay below the upper LIM
461 confidence interval for decadal to multidecadal periods. However, poor reproducibility
462 between the various PDO reconstructions (Fig 5d) calls into question their collective
463 fidelity as paleo-PDO indices. Beyond profound differences in the various proxy
464 networks, the reconstructions also reflect differences in how well local climate responds
465 to large-scale atmospheric variability, potential seasonal biases, and geographic domain
466 (e.g., Tingley, 2012; St. George, 2014). As most PDO reconstructions are based on tree
467 ring width timeseries, the statistical removal of growth-related trends in these series
468 (Cook et al., 1995; Jones et al., 2009 and references therein) may deflate centennial-scale
469 variability, causing a loss of spectral power at the lowest frequencies in Fig. 5c.

470 As the PDO represents not one but many dynamical processes, it poses a unique
471 challenge as a target for proxy-based reconstruction. The 20th century PDO index has
472 contributions from different processes with varying relative amplitudes and phases (cf.
473 Fig. 3). If the relative importance of these contributions varies, then the apparent
474 teleconnection from their sum (the PDO) could be non-stationary *even if teleconnections*
475 *related to the individual PDO processes were fixed.* Moreover, we might expect different
476 proxy networks sensitive to different PDO processes (i.e. tropical versus extratropical

sources of PDO variability) to yield different PDO reconstructions through time. Additionally, some proxies could be strongly correlated with the PDO less because they are directly influenced by it than because they are also "climate integrators" acting to redden their own forcing by ENSO, as the North Pacific Ocean does (Newman et al. 2003; see also Pederson et al., 2011).

Given that coupled ocean-atmosphere dynamics give rise to the PDO, high-resolution SST reconstructions are particularly important inputs to reconstructed fields. Many SST-sensitive coral oxygen isotope records span the tropical Pacific, often extending into the late 19th century, but such records also reflect changes in the oxygen isotopic content of seawater, largely correlated with salinity (Fairbanks et al., 1997; Conroy et al., 2013). As such, SST-only proxies in corals, such as coral Sr/Ca ratios, hold promise in delivering constraints on past SST, as well as past salinity, when combined with coral oxygen isotope records (i.e. Nurhati et al., 2011).

Innovative new approaches aimed at reconstructing different components of the PDO illustrate the benefits of expanding the available network of PDO-related proxies (e.g., McCabe-Glynn et al. 2013; Emile-Geay et al., 2013; D'Arrigo et al. 2014). As it stands, the current disagreement amongst PDO reconstructions is problematic for any assessment of PDO impacts over the last several hundred years (Kipfmueller et al. 2012).

PDO Climate Impacts

In this section, we address both forecasting the PDO, and forecasting with the PDO, focusing on the need to distinguish between PDO-correlated and PDO-predictable climate impacts.

RETROSPECTIVE ANALYSIS OF PDO IMPACTS

PDO dependence on other climate processes implies that correlations with the PDO will be related to correlations with other climate indices. For example, Fig. 5 shows the correlation of revised United States climate division (nClimDiv; Vose et al 2014) cold-season precipitation anomalies with the PDO, ENSO, and NPI indices. While there are some interesting differences, these maps are clearly all quite similar, with ENSO having the most pronounced signal. PDO and ENSO correlations with year-round Palmer Drought Severity Index (PDSI) are also similar except perhaps in the Northwest; for cold-season temperatures, while differences between PDO and ENSO correlations are nontrivial, by far the strongest correlations are with the NPI (Fig. S6). A key concern then is to determine *additional* predictive information from the PDO, and not merely duplicate teleconnections from those processes that *simultaneously* act to force it.

Many studies that have explored historical PDO relationships with climate, especially hydrological quantities including precipitation, snowpack, streamflow, and drought (eg, Gershunov and Barnett 1998; Hamlet and Lettenmaier 1999; McCabe and Dettinger 1999, 2002; Gutzler et al. 2002; Brown and Comrie 2004; McCabe et al. 2004; Stewart et al. 2005; Hunter et al. 2006; Kurtzman and Scanlon 2007; Yu and Zwiers 2007; Higgins et al. 2007; Hu and Huang 2009; Zhang et al. 2010; Goodrich and Walker 2011; Mehta et al. 2012; Li et al. 2012; ; McCabe et al. 2012; Cook et al. 2014; Oakley and Redmond 2014; Wang et al. 2014), are often focused on the impact of PDO phase on ENSO teleconnections. However, sorting ENSO responses by PDO phase may have unanticipated pitfalls beyond double counting. On average, well over half of the large-scale extratropical atmospheric seasonal-mean anomaly occurring during an ENSO event

522 is a consequence not of ENSO, but rather of ever-present weather and internal slowly-
523 evolving atmospheric anomalies (e.g., blocking). This "ENSO-year/but-non-ENSO-
524 forced" atmospheric anomaly also modifies North Pacific SSTAs through changes in
525 surface fluxes, while simultaneously contributing to the seasonal-mean climate anomaly
526 downstream over North America (Pierce 2002). [Obviously, such anomalies exist in non-
527 ENSO years as well; cf. NPI and PDO temperature correlations in Fig. S6.] Additionally,
528 like snowflakes no two ENSO events are alike; recent research (see review by Capotondi
529 et al. 2015) suggests that "diversity" between ENSO events may also drive different
530 and/or asymmetric teleconnections across the North Pacific into North America (eg.,
531 Hoerling et al. 2001; Larkin and Harrison 2005; Wu et al. 2005; Mo 2010; Yu et al 2012).
532 Of course, different teleconnections could drive variations in the atmospheric bridge with
533 consequent PDO variations (eg, An et al. 2007; Yeh et al. 2015), including on decadal
534 time scales (Yeh and Kirtman 2008). ENSO diversity is evident in separate ENSO SST
535 composites based on high/low PDO years (see Fig. S7; also cf. the North Pacific SSTAs
536 for the two ENSO eigenmodes in Figs. 3d and f), suggesting that this stratification may
537 partly capture ENSO diversity impacts on both PDO and ENSO teleconnections, rather
538 than PDO impacts on ENSO teleconnections.

539 PDO PREDICTION

540 Interest in PDO prediction is high due to its potential climate impacts, especially
541 related to decadal variation and PDO regime shifts. From the earlier discussion, however,
542 we might expect that predicting regime duration, which may depend upon the current
543 amplitude of different processes with different memory time scales, could be more
544 skillful than predicting regime shifts, which may be largely randomly forced.

Some extended forecast skill resulting from oceanic Rossby wave propagation (Schneider and Miller 2001) may occur for western Pacific SSTAs within the SAFZ. Recent studies established multi-year predictability of the Kuroshio extension speed (Nonaka et al. 2012) and stability (Qiu et al. 2014) that enter the PDO forcing F in equation (1). How much this enhances PDO predictability (cf. Figs. 2e, 2f) remains to be determined, but it may be related to the more slowly evolving "North Pacific" component in Fig. 3.

Given the PDO's relationship with ENSO, PDO forecast skill strongly depends on ENSO forecast skill, especially for forecast leads of up to 1-2 years (eg, Alexander et al. 2008b; Wen et al. 2012). For longer forecast leads, largely unpredictable ENSO events act mostly as high amplitude noise for decadal forecasts (Newman 2013; Wittenberg et al. 2014). This may help explain why decadal PDO forecast skill in CMIP5 hindcasts is unimpressive (Guemas et al. 2012; Kim et al. 2012; van Oldenborgh et al. 2012; Newman 2013; Meehl and Teng 2014), although model bias also contributes (Guemas et al. 2012; Kim et al. 2014). Similarly, predicting the atmospheric impacts associated with the PDO may largely depend upon tropical forecast skill. In fact, current GCM forecasts initialized with a PDO SSTA alone have little skill (Kumar et al. 2013; Kumar and Wang 2014), although additional skill with higher resolution models remains possible (eg, Jung et al. 2012).

PDO IMPACTS ON MARINE ECOSYSTEMS

As an imprint on SST of multiple processes driving a coherent large-scale low-frequency structure in the ocean, the PDO organizes ocean biological responses across the Pacific basin. Many studies show a correlation between the PDO index and ocean

568 ecosystem variables, particularly in the context of ecosystem regime shifts (e.g.,
569 Anderson and Piatt 1999; Hare and Mantua 2000; Miller and Schneider 2000). However,
570 it may be more important, although difficult, to go beyond these correlations and connect
571 specific ecosystem responses to the relevant PDO physical processes, including the
572 thermal structure of the upper-ocean, thermocline depth, vertical mixing and upwelling,
573 transport by mean currents, and transport by eddies. For example, sub-surface
574 thermocline changes correlated with PDO can affect bottom-dwelling (benthic) fish and
575 invertebrate communities on the shelf and migrating upper-ocean (pelagic) communities
576 of the deep waters differently. The thermocline response may be dominated by Ekman
577 pumping and driven by wind-stress curl rather than direct surface heat-fluxes that drive
578 SST. Copepods, a key type of ocean zooplankton, closely correspond with PDO
579 variations in the northern California Current (Peterson and Keister 2003), with cold water
580 periods (negative PDO) yielding a lipid-rich, sub-arctic (cold-water) zooplankton
581 community associated with high production of West Coast salmon (Peterson and
582 Schwing 2003). The suggested mechanism linking PDO to these zooplankton is change
583 in the transport of subarctic vs. subtropical water masses driven by PDO-related
584 atmospheric forcing (Keister et al. 2011; Bi et al. 2011). Related to this is the Double
585 Integration Hypothesis (Di Lorenzo and Ohman 2013), whereby a particular species of
586 southern California Current zooplankton appears to integrate PDO-related transport,
587 while the transport integrates PDO-related atmospheric forcing. Changes in the strength
588 of the Kuroshio/Oyashio Extension, related to gyre-scale adjustment processes due to
589 PDO-related atmospheric forcing (Miller et al. 2004), control variability in warm and
590 cold water zooplankton (Chiba et al. 2013).

591 Alternating multi-decadal biomass fluctuations of sardines and anchovies in the
592 Kuroshio/Oyashio Extension, the California Current System, and the Humboldt Current
593 System, have varied in concert with low-frequency variations of the PDO since the early
594 twentieth century (Yasuda et al. 1999; Chavez et al. 2003). These alternating variations
595 may be related to stock-specific optimal thermal windows for larval-stage survival rates
596 (Takasuka et al., 2008), which in turn support strong correlations between recruitment
597 and regional SSTs in PDO-affected regions (Lindegren et al. 2013).
598 A unique case is the PDO impact on Pacific salmon populations, since salmon
599 spend part of their lives in fresh water and part in the ocean. During salmon fresh water
600 periods, stream flow and stream temperature, which can be influenced by PDO-related
601 atmospheric forcing patterns (Mantua et al. 1997), may influence juvenile salmon growth
602 and survival rates, and spawning success for adults (Schindler and Rogers 2009). At sea,
603 the oceanic response to PDO forcing may alter food availability and predation through
604 various physical processes related to upwelling, ocean stratification, coastal current
605 flows, and upper-ocean temperatures (Gargett 1997). Since the PDO forcing functions
606 extend from Alaska to California and across the Pacific to East Asia, the imprint of the
607 PDO forcing functions on land and at sea can organize the salmon populations in widely
608 different ways, producing synchrony or asynchrony across basin-scales (e.g., Beamish
609 and Bouillon 1993; Francis and Hare 1994; Mantua et al. 1997; Hare et al. 1999, Stachura
610 et al. 2013).
611 Some ecosystems may exhibit a response to PDO physical processes that have
612 greater predictability than the PDO index itself, such as in the Kuroshio Extension region
613 where the regional ecosystem (Chiba et al. 2013) is sensitive to SST, vertical nutrient

614 fluxes, and horizontal transport. Another possibility is the influence of PDO forcing
615 functions causing changes in ocean eddy statistics that are correlated to PDO. These eddy
616 changes can either persist or propagate into different biogeographic regions over many
617 months. In simulations of the California Current System, large-scale winds correlated
618 with the Aleutian Low have been found to cause changes in eddy variance that could
619 influence vertical mixing, lateral mixing, or retention over the shelf (Di Lorenzo et al.
620 2013). Also, even if PDO climate regime "shifts" are due to random superpositions of
621 PDO processes, ecological regimes may still occur for those biological systems with a
622 nonlinear sensitivity to climate (eg, Steele 2004; Hsieh et al. 2005; Overland et al. 2010).
623 Additional research is required to sort out all the possible ways that PDO-correlated
624 physical forcing can impact biology.

625 **Conclusion**

626 The PDO is now a well-established climate index, frequently used in correlation
627 analyses to suggest physical linkage between a particular variable of interest (e.g.,
628 phytoplankton, grain production, rainfall, extreme wind events, etc.) and North Pacific
629 ocean variability. As summarized in Fig. 7, the PDO represents not a single phenomenon
630 but rather a combination of processes that span the Tropics and extratropics. It is
631 therefore important to distinguish climate impacts *correlated* with the PDO from climate
632 impacts that are *predictable* by the PDO. In this context, since much of the PDO
633 represents the oceanic response to atmospheric forcing, care should be taken when using
634 the PDO as a "forcing" function of non-oceanic responses without a convincing argument
635 for the physical forcing mechanism. For example, claiming that PDO "drives"
636 contemporaneous changes in rainfall over western North America (e.g., Gershunov and

637 Barnett 1998) is more simply explained by both variables (PDO and rainfall) being
638 driven by a common forcing function (Pierce, 2002) such as ENSO and internal
639 variability of the mid-latitude atmosphere. A "common forcing function" must therefore
640 be considered as the first approximation for explaining a discovered simultaneous
641 correlation between non-oceanic variables and PDO. Caution is also needed when using
642 the PDO together with other indices in analyses where the PDO depends upon those
643 indices; determining which portion of the PDO, and/or which PDO process, is
644 legitimately an “independent” predictor is an important first step.
645 Ultimately, numerical integration may offer the best hope for establishing links
646 with the PDO, because the historical record of PDO has too few degrees of freedom to
647 ascribe significance to a lagged relation, a consequence of PDO representing an
648 "integrated in time" (low-pass filtered) response to atmospheric forcing. Of course, the
649 issues presented above still need consideration when analyzing model output (eg, Polade
650 et al. 2013). Moreover, a realistic balance of PDO processes must be simulated in
651 CGCMs. Models with particularly weak tropical-PDO connections may be ill-suited for
652 examination of the importance of tropical forcing to the North Pacific (e.g., Giannakis
653 and Majda 2012). In fact, (3) may be one good approach for process-based analysis of
654 CMIP CGCMs, since it tests not only how well ENSO variability is captured but also
655 how ENSO teleconnections and North Pacific memory and dynamical processes are
656 simulated.
657

REFERENCES

Alexander, M. A., 1990: Simulation of the response of the North Pacific Ocean to the anomalous atmospheric circulation associated with El Nino. *Clim. Dyn*., **5**, 53–65.

Alexander, M. A., 1992: Midlatitude atmosphere-ocean interaction during El Nino. Part I: The North Pacific Ocean, *J. Clim*., **5**, 944 – 958.

Alexander, M., 2010: Extratropical air-sea interaction, sea surface temperature variability, and the Pacific Decadal Oscillation. Vol. 189 of *Geophysical Monograph Series*, American Geophysical Union, Washington, D. C., 123–148.

Alexander, M., I. Bladé, M. Newman, J. R. Lanzante, N.-C. Lau, and J. D. Scott, 2002: The Atmospheric Bridge: The Influence of ENSO Teleconnections on Air–Sea Interaction over the Global Oceans. *J. Climate*, **15**, 2205–2231.

Alexander, M., A. Capotondi, A. Miller, F. Chai, R. Brodeur and C. Deser, 2008a: Decadal variability in the Northeast Pacific in a physical-ecosystem model: Role of mixed layer depth and trophic interactions. *Journal of Geophysical Research-Oceans,* **113**, C02017, doi:10.1029/2007JC004359.

Alexander, M. A., and C. Deser, 1995: A mechanism for the recurrence of wintertime midlatitude SST anomalies. *J. Phys. Oceanogr.*, **25**, 122–137.

Alexander, M. A., C. Deser, and M. S. Timlin, 1999: The re-emergence of SST anomalies in the North Pacific Ocean. *J. Climate*, **12**, 2419–2431.

Alexander, M. A., N.-C. Lau, and J. D. Scott, 2004: Broadening the atmospheric bridge paradigm: ENSO teleconnections to the North Pacific in summer and to the tropical west Pacific-Indian oceans over the seasonal cycle. In *Earth's Climate: The Ocean-*

Atmosphere Interaction, edited by Geophys. Monogr. Ser., vol. 147, edited by C. Wang, S.-P. Xie, and J. A. Carton, pp. 85– 104, AGU, Washington, D. C..

Alexander, M. A., L. Matrosova, C. Penland, J. D. Scott, and P. Chang, 2008b: Forecasting Pacific SSTs: Linear Inverse Model Predictions of the PDO. *J. Climate*, **21**, 385-402.

Alexander, M., and J. D. Scott, 2008: The Role of Ekman Ocean Heat Transport in the Northern Hemisphere Response to ENSO. *J. Climate*, **21**, 5688–5707, doi:10.1175/2008JCLI2382.1.

Alexander, M. A., M. S. Timlin, and J. D. Scott, 2001: Winter-to- winter recurrence of sea surface temperature, salinity and mixed layer depth anomalies. *Prog. Oceanogr.,* **49**, 41–61.

An, S. I., J.-S. Kug, A. Timmermann, I.-S. Kang, and O. Timm, 2010: The Influence of ENSO on the Generation of Decadal Variability in the North Pacific. *J. Climate*, **20**, 667–680, doi:10.1175/JCLI4017.1.

Anderson, P.J., and J.F. Piatt, 1999: Community reorganization in the Gulf of Alaska following ocean climate regime shift. *Mar. Ecol. Prog. Ser.*, **189** (26), 117-123.

Ault, T., C. Deser, M. Newman, and J. Emile-Geay, 2013: Characterizing decadal to centennial variability in the equatorial Pacific during the last millennium. *Geophys. Res. Lett*, **40**, 3450-3456, doi:10.1002/grl.50647.

Barlow, M., S. Nigam, and E. H. Berbery, 2001: ENSO, Pacific Decadal Variability, and U.S. Summertime Precipitation, Drought, and Stream Flow. *J. Climate*, **14**, 2105–2128.

Barsugli, J. J. and D. S. Battisti, 1998: The basic effects of atmosphere-ocean thermal coupling on midlatitude variability. *J. Atmos. Sci*., **55**, 477-493.

703 Beamish, R. J. and D.R. Bouillon, 1993: Pacific salmon production trends in relation to
704 climate. *Can. J. Fish. Aquat. Sci.*, **50**, 1002-1016.
705 Beran, J., 1994: *Statistics for long-memory processes*. Chapman and Hall, New York, 315
706 pp.
707 Bhatt, U. S., M. A. Alexander, D. S. Battisti, D. D. Houghton, and L. M. Keller, 1998:
708 Atmosphere-ocean interaction in the North Atlantic: Near-surface climate variability. *J.*
709 *Clim*., **11**, 1615 – 1632.
710 Bi, H., W. T. Peterson, and P. T. Strub, 2011: Transport and coastal zooplankton
711 communities in the northern California Current system. *Geophys. Res. Lett*., **38**, L12607,
712 doi:10.1029/2011GL047927
713 Biondi, F., A. Gershunov, and D. R. Cayan, 2001: North Pacific Decadal Climate
714 Variability since 1661. *J. Climate*, 14, 5–10.
715 Bladé, I., 1997: The influence of midlatitude coupling on the low- frequency variability
716 of a GCM. Part I: No tropical SST forcing. *J. Clim*., **10**, 2087–2106.
717 Brown, D. P., and A. C. Comrie, 2004: A winter precipitation “dipole” in the western
718 United States associated with multidecadal ENSO variability. *Geophys. Res. Lett*, **31**,
719 L09203, doi:10.1029/2003GL018726.
720 Capotondi, A., A. T. Wittenberg, M. Newman, E. Di Lorenzo, J.-Y. Yu, P. Braconnot, J.
721 Cole, B. Dewitte, B. Giese, E. Guilyardi, F.-F. Jin, K. Karnauskas, B. Kirtman, T. Lee, N.
722 Schneider, Y. Xue, and S.-W. Yeh, 2015: Understanding ENSO diversity. *Bull. Amer.*
723 *Meteor. Soc.*, in press.
724 Carton, J.A., and B.S. Giese, 2008: A reanalysis of ocean climate using Simple Ocean
725 Data Assimilation (SODA). *Mon. Wea. Rev.,* **136**, 2999-3017.

726 Cayan, D.R., 1992: Latent and sensible heat flux anomalies over the northern oceans: The
727 connection to monthly atmospheric circulation. *J. Clim*., **5**, 354–369.
728 Chavez, F. P., Ryan, J., Lluch-Cota, S. E., & Niquen, M. C., 2003: From anchovies to
729 sardines and back: Multi-decadal change in the Pacific Ocean. *Science*, **299**, 217–221.
730 Chiang, J. C. H., and D. J. Vimont, 2004: Analagous meridional modes of atmosphere-
731 ocean variability in the tropical Pacific and tropical Atlantic. *J. Climate*, **17**(21), 4143–
732 4158.
733 Chiba, S., E. Di Lorenzo, A. Davis, J. E. Keister, B. Taguchi, Y. Sasai, and H. Sugisaki,
734 2013: Large-scale climate control of zooplankton transport and biogeography in the
735 Kuroshio-Oyashio Extension region. *Geophys. Res. Lett*., **40**, 5182–5187.
736 Compo, G., and P.D. Sardeshmukh, 2010: Removing ENSO-related variations from the
737 climate record. *J. Climate*, **23**, 1957-1978. DOI: 10.1175/2009JCLI2735.1
738 Conroy, J.L., K.M. Cobb, J. Lynch-Stieglitz, and P. Polissar, 2014: Constraints on the
739 salinity-oxygen isotope relationship in the central tropical Pacific Ocean. *Marine*
740 *Chemistry* doi: 10.1016/j.marchem.2014.02.001.
741 Cook, B. I., J. E. Smerdon, R. Seager, and E. R. Cook, 2014: Pan-Continental Droughts
742 in North America over the Last Millennium. *J. Climate*, **27**, 383–397, doi:10.1175/JCLI-
743 D-13-00100.1.
744 Cook, E. R., K. R. Briffa, D. M. Meko, D. A. Graybill, and G. Funkhouser, 1995: The
745 segment length curse in long tree-ring chronology development for paleoclimatic studies.
746 *Holocene*, **5**, 229–237.
747 Dai, A., 2012: The influence of the inter-decadal Pacific oscillation on US precipitation
748 during 1923–2010. *Clim Dyn*, doi:10.1007/s00382-012-1446-5.

749 Davis, R.E., 1976: Predictability of Sea Surface Temperature and Sea Level Pressure
750 Anomalies over the North Pacific Ocean. *J. Phys. Oceanogr.*, **6**, 249–266.
751 Deser, C., M. A. Alexander, and M. S. Timlin, 1999: Evidence for wind-driven
752 intensification of the Kuroshio Current Extension from the 1970s to the 1980s. *J. Clim.*,
753 **12**, 1697–1706.
754 Deser, C., A. S. Phillips, and J. W. Hurrell, 2004: Pacific Interdecadal Climate
755 Variability: Linkages between the Tropics and the North Pacific during Boreal Winter
756 since 1900. *J. Climate*, **17**, 3109–3124.
757 Deser, C., and Coauthors, 2012: ENSO and Pacific Decadal Variability in the
758 Community Climate System Model Version 4. *J. Climate*, **25**, 2622–2651,
759 doi:10.1175/JCLI-D-11-00301.1.
760 Deser, C., and M. L. Blackmon, 1995: On the Relationship between Tropical and North
761 Pacific Sea Surface Temperature Variations. *J. Climate*, **8**, 1677–1680.
762 Deser, C., M. Alexander, and M. S. Timlin, 2003: Understanding the Persistence of Sea
763 Surface Temperature Anomalies in Midlatitudes. *J. Climate* **16**, 57–72.
764 Deser, C., and M. Timlin, 1998: Atmosphere-ocean interaction on weekly timescales in
765 the North Atlantic and Pacific. *J. Climate*, 10, 393-408.
766 Di Lorenzo, E., and M.D. Ohman, 2013: A double-integration hypothesis to explain
767 ocean ecosystem response to climate forcing. *Proceedings Of The National Academy Of*
768 *Sciences*, **110** (7), 2496-2499.
769 D'Arrigo, R., R. Villalba, and G. Wiles, 2001: Tree-ring estimates of Pacific decadal
770 climate variability. *Clim Dyn*, **18**, 219–224, doi:10.1007/s003820100177.

771 D'Arrigo, R., and R. Wilson, 2006: On the Asian expression of the PDO. *Int. J. Climatol*,
772 **26**, 1607–1617, doi:10.1002/joc.1326.
773 D'Arrigo, R., R. Wilson, G. Wiles, K. Anchukaitis, O. Solomina, N. Davi, C. Deser, and
774 E. Dolgova, 2014: Tree‐ring reconstructed temperature index for coastal northern Japan:
775 implications for western North Pacific variability. *Int. J. Climatol*, n/a–n/a,
776 doi:10.1002/joc.4230.
777 Ebbesmeyer, C. C., D. R. Cayan, D. R. McLain, F. H. Nichols, D. H. Peterson, and K. T.
778 Redmond, 1991: 1976 step in the Pacific climate: Forty environmental changes between
779 1968–1975 and 1977–1985. Proc. Seventh Annual Pacific Climate Workshop, Asilomar,
780 CA, California Dept. of Water Research, 115–126.
781 Fairbanks, R. G., M. N. Evans, J. L. Rubenstone, R. A. Mortlock, K. Broad, M. D.
782 Moore, and C. D. Charles, 1997: Evaluating climate indices and their geochemical
783 proxies measured in corals. *Coral Reefs*, **16**(suppl.), S93 – S100.
784 Felis, T., A. Suzuki, H. Kuhnert, N. Rimbu, and H. Kawahata, 2010: Pacific Decadal
785 Oscillation documented in a coral record of North Pacific winter temperature since 1873.
786 *Geophys. Res. Lett.*, **37**, n/a–n/a, doi:10.1029/2010GL043572.
787 Fleming, S. W., 2009: Exploring the nature of Pacific climate variability using a "toy"
788 nonlinear stochastic model. *Can. J. Phys*, **87**, 1127–1131, doi:10.1139/P09-095.
789 Fleming, S. W., 2014: A non-uniqueness problem in the identification of power-law
790 spectral scaling for hydroclimatic time series. *Hydrological Sciences Journal*, **59**, 73–84,
791 doi:10.1080/02626667.2013.851384.
792 Folland, C. K., 2008: Interdecadal Pacific Oscillation Time Series. Web document
793 retrieved from http://www.iges.org/c20c/IPO_v2.doc.

794 Folland, C. K., J. A. Renwick, M. J. Salinger, and A. B. Mullan, 2002: Relative
795 influences of the Interdecadal Pacific Oscillation and ENSO on the South Pacific
796 Convergence Zone. *Geophys. Res. Lett*, **29**, 1643, doi:10.1029/2001GL014201.
797 Fraedrich, K., U. Luksch, and R. Blender, 2004: 1/*f* model for long-time memory of the
798 ocean surface temperature. *Phys. Rev. E*, **70**, 037301, doi:10.1103/PhysRevE.70.037301.
799 Francis, R.C., and S.R. Hare, 1994: Decadal-scale regime shifts in the large marine
800 ecosystems of the north-east Pacific: a case for historical science. *Fisheries*
801 *Oceanography* **3**, 279–291.
802 Frankignoul, C., and K. Hasselmann, 1977: Stochastic climate models. Part II:
803 Application to sea-surface temperature anomalies and thermocline variability. *Tellus*, **29**,
804 284–305.
805 Frankignoul, C., P. Müller, and E. Zorita, 1997: A Simple Model of the Decadal
806 Response of the Ocean to Stochastic Wind Forcing. *J. Phys. Oceanogr.*, **27**, 1533–1546.
807 Frankignoul, C., and R. W. Reynolds, 1983: Testing a dynamical model for mid-latitude
808 sea surface temperature anomalies. *J. Phys. Oceanogr*., **13**, 1131–1145.
809 Frankignoul, C., N. Sennechael, Y. Kwon, and M. Alexander, 2011: Influence of the
810 meridional shifts of the Kuroshio and the Oyashio Extensions on the atmospheric
811 circulation. *J. Climate*, **24**, 762–777.
812 Furtado, J. C., E. Di Lorenzo, N. Schneider, and N. A. Bond, 2011: North Pacific
813 Decadal Variability and Climate Change in the IPCC AR4 Models. *J. Climate*, **24**, 3049–
814 3067, doi:10.1175/2010JCLI3584.1.
815 Gargett, A. E., 1997: The optimal stability “window”: a mechanism underlying
816 383 decadal fluctuations in North Pacific salmon stocks. *Fish. Oceanogr*. **6**, 1-9.

817 Gershunov, A., and T. P. Barnett, 1998: Interdecadal Modulation of ENSO
818 Teleconnections. *Bull. Amer. Meteor. Soc*, **79**, 2715–2725, doi:10.1175/1520-
819 0477(1998)079<2715:IMOET>2.0.CO;2.
820 Giannakis, D., and A. J. Majda, 2012: Limits of predictability in the North Pacific sector
821 of a comprehensive climate model. *Geophys. Res. Lett*, **39**, n/a–n/a,
822 doi:10.1029/2012GL054273.
823 Goodrich, G. B., and J. M. Walker, 2011: The Influence of the PDO on Winter
824 Precipitation During High- and Low-Index ENSO Conditions in the Eastern United
825 States. *Physical Geography*, **32**, 295–312, doi:10.2747/0272-3646.32.4.295.
826 Graham, N. E., 1994: Decadal-scale climate variability in the 1970s and 1980s:
827 Observations and model results. *Climate Dyn*., **10**, 135–159.
828 Granger, C. W. J., 1980: Long memory relationships and the aggregation of dynamic
829 models. *Journal of Econometrics*, **14**, 227–238.
830 Guan, B., and S. Nigam, 2008: Pacific Sea Surface Temperatures in the Twentieth
831 Century: An Evolution-Centric Analysis of Variability and Trend. *J. Climate*, **21**, 2790–
832 2809, doi:10.1175/2007JCLI2076.1.
833 Guemas, V., F. J. Doblas-Reyes, F. Lienert, Y. Soufflet, and H. Du, 2012: Identifying the
834 causes of the poor decadal climate prediction skill over the North Pacific. *J. Geophys.*
835 *Res*, **117**, n/a–n/a, doi:10.1029/2012JD018004.
836 Gutzler, D. S., D. M. Kann, and C. Thornbrugh, 2002: Modulation of ENSO-Based
837 Long-Lead Outlooks of Southwestern U.S. Winter Precipitation by the Pacific Decadal
838 Oscillation. *Weather and Forecasting*, **17**, 1163–1172.

839 Hamlet, A.F., and D.P. Lettenmaier, 1999: Columbia River streamflow forecasting based
840 on ENSO and PDO climate signals. *J Water Res Pl*, **125**, 333-341.
841 Hanawa, K., and S. Sugimoto, 2004: 'Reemergence'areas of winter sea surface
842 temperature anomalies in the world's oceans. *Geophys. Res. Lett*., **31**, L10303,
843 doi:10.1029/2004GL019904.
844 Hare, S.R., and N.J. Mantua, 2000: Empirical evidence for North Pacific regime shifts in
845 1977 and 1989. *Prog. Oceanogr.*, 47 (2-4), 103-145.
846 Hare, S.R., N.J. Mantua, and R.C. Francis, 1999: Inverse production regimes: Alaskan
847 and West Coast Pacific Salmon. *Fisheries*, **21**, 6-14.
848 Hasselmann, K., 1976: Stochastic climate models. Part I. Theory. *Tellus*, **28**, 474—485.
849 Higgins, R. W., V. B. S. Silva, W. Shi, and J. Larson, 2007: Relationships between
850 Climate Variability and Fluctuations in Daily Precipitation over the United States. *J.*
851 *Climate*, **20**, 3561–3579, doi:10.1175/JCLI4196.1.
852 Hoerling, M. P., A. Kumar, and T. Xu, 2001: Robustness of the Nonlinear Climate
853 Response to ENSO's Extreme Phases. *J. Climate*, **14**, 1277–1293.
854 Hsieh, C.-H., S. M. Glaser, A. J. Lucas, and G. Sugihara, 2005: Distinguishing random
855 environmental fluctuations from ecological catastrophes for the North Pacific Ocean.
856 *Nature*, **435**, 336–340, doi:10.1038/nature03553.
857 Hu, Z.-Z., and B. Huang, 2009: Interferential Impact of ENSO and PDO on Dry and Wet
858 Conditions in the U.S. Great Plains. *J. Climate*, **22**, 6047–6065,
859 doi:10.1175/2009JCLI2798.1.

860 Ishii, M., A. Shouji, S. Sugimoto, and T. Matsumoto, 2005: Objective Analyses of Sea-
861 Surface Temperature and Marine Meteorological Variables for the 20th Century using
862 ICOADS and the Kobe Collection. *Int. J. Climatol*., **25**, 865-879.
863 Iwasaka, N., and J. M. Wallace, 1995: Large scale air sea inter- action in the Northern
864 Hemisphere from a view point of variations of surface heat flux by SVD analysis. *J.*
865 *Meteorol. Soc. Jpn*., **73**, 781–794.
866 Jones, P.D. et al., 2009: High-resolution paleoclimatology of the last millennium: a
867 review of current status and future prospects. *Holocene* **19**(1), 3-49.
868 Jung, T. and co-authors, 2012: High-resolution global climate simulations with the
869 ECMWF model in Project Athena: Experimental design, model climate and seasonal
870 forecast skill. *J. Climate*, **25**, 3155-3172.
871 Kaplan, A., M. Cane, Y. Kushnir, A. Clement, M. Blumenthal, and B. Rajagopalan,
872 1998: Analyses of global sea surface temperature 1856-1991. *Journal of Geophysical*
873 *Research*, **103**, 18,567-18,589.
874 Keister, J.E., E. Di Lorenzo, C.A. Morgan, V. Combes, W.T. Peterson, 2011:
875 Zooplankton species composition is linked to ocean transport in the Northern California
876 Current. *Global Change Biology*, **17**, 2498-2511.
877 Kelly, K.A., R.J. Small, R.M. Samelson, B. Qiu, T.M. Joyce, Y.-O. Kwon and M.F.
878 Cronin, 2010: Western boundary currents and frontal air-sea interaction: Gulf Stream and
879 Kuroshio Extension. *J. Climate*, **23**, 5644-5667.
880 Keshner, M. S., 1982: 1/f Noise. *Proceedings of the IEEE*, **70**, 212.
881 Kim, H.-M., P. J. Webster, and J. A. Curry, 2012: Evaluation of short-term climate

882 change prediction in multi-model CMIP5 decadal hindcasts, *Geophys. Res. Lett.*, **39**,
883 L10701, doi:10.1029/2012GL051644.
884 Kim, H. M., Y. G. Ham, and A. A. Scaife, 2014: Improvement of initialized decadal
885 predictions over the North Pacific Ocean by systematic anomaly pattern correction. *J.*
886 *Climate*, **27** (13), 5148-5162.
887 Kipfmueller, K. F., E. R. Larson, and S. St George, 2012: Does proxy uncertainty affect
888 the relations inferred between the Pacific Decadal Oscillation and wildfire activity in the
889 western United States? Geophys. Res. Lett, 39, n/a–n/a, doi:10.1029/2011GL050645.
890 Klein, S. A., D. L. Hartmann, and J. R. Norris, 1995: On the relationships among low-
891 cloud structure, sea surface temperature, and atmospheric circulation in the summertime
892 northeast Pacific. *J. Climate*, **8**, 1140–1155.
893 Kumar, A., and H. Wang, 2014: On the potential of extratropical SST anomalies for
894 improving climate predictions. *Clim Dyn*, 1–13, doi:10.1007/s00382-014-2398-8.
895 Kumar, A., H. Wang, W. Wang, Y. Xue, and Z.-Z. Hu, 2013: Does Knowing the Oceanic
896 PDO Phase Help Predict the Atmospheric Anomalies in Subsequent Months? *J. Climate*,
897 **26**, 1268–1285, doi:10.1175/JCLI-D-12-00057.1.
898 Kurtzman, D., and B. R. Scanlon, 2007: El Nino–Southern Oscillation and Pacific
899 Decadal Oscillation impacts on precipitation in the southern and central United States:
900 Evaluation of spatial distribution and predictions. *Water Resour. Res.*, **43**, W10427,
901 doi:10.1029/2007WR005863.
902 Kushnir, Y., W. A. Robinson, I. Bladé, N. M. J. Hall, S. Peng, and R. Sutton, 2002:
903 Atmospheric response to extratropical SST anomalies: Synthesis and evaluation. *J. Clim.*,
904 **15**, 2205 – 2231.

905 Kwon, Y., M. Alexander, N. Bond, C. Frankignoul, H. Nakamura, B. Qiu, and L.
906 Thompson, 2010: Role of the Gulf Stream and Kuroshio–Oyashio systems in large-scale
907 atmosphere–ocean interaction: A review. *J. Climate*, **23**, 3249–3281.
908 Kwon, Y.-O., and C. Deser, 2007: North Pacific Decadal Variability in the Community
909 Climate System Model Version 2. *J. Climate*, **20**, 2416–2433, doi:10.1175/JCLI4103.1.
910 Laepple, T., and P. Huybers, 2014: Global and regional variability in marine surface
911 temperatures. *Geophys. Res. Lett*, **41**, 2528–2534, doi:10.1002/2014GL059345.
912 Larkin, N. K., and D.E., Harrison, 2005: On the definition of El Niño and associated
913 seasonal average U.S. weather anomalies. *Geophys. Res. Lett*., **32**, L13705,
914 doi:10.1029/2005GL022738.
915 Latif, M., and T. P. Barnett, 1994: Causes of decadal climate variability over the North
916 Pacific and North America. *Science*, **266**, 634–637.
917 Latif, M., and T. P. Barnett, 1996: Decadal climate variability over the North Pacific and
918 North America: Dynamics and predictability. *J. Clim*., **9**, 2407–2423.
919 Lau, N. C., and M. J. Nath, 1994: A modeling study of the relative roles of tropical and
920 extratropical SST anomalies in the variability of the global atmosphere-ocean system. *J.*
921 *Clim*., **7**, 1184–1207.
922 Lau, N.-C., and M. J. Nath, 1996: The role of the "atmospheric bridge" in linking tropical
923 Pacific ENSO events to extratropical SST anomalies. *J. Clim*., **9**, 2036–2057.
924 Lau, N.-C., and M. J. Nath, 2001: Impact of ENSO on SST variability in the North
925 Pacific and North Atlantic: Seasonal dependence and role of extratropical air-sea
926 coupling. *J. Clim*., **14**, 2846–2866.

927 Li, L., W. Li, and Y. Kushnir, 2012: Variation of the North Atlantic subtropical high
928 western ridge and its implication to Southeastern US summer precipitation. *Clim Dyn*, **39**,
929 1401–1412, doi:10.1007/s00382-011-1214-y.
930 Lienert, F., J. C. Fyfe, and W. J. Merryfield, 2011: Do Climate Models Capture the
931 Tropical Influences on North Pacific Sea Surface Temperature Variability? *J. Climate*,
932 **24**, 6203–6209, doi:10.1175/JCLI-D-11-00205.1.
933 Lindegren, M., D.M. Checkley, T. Rouyer, A.D. MacCall, N.C. Stenseth, 2013: Climate,
934 fishing, and fluctuations of sardine and anchovy in the California Current. *Proc. Nat.*
935 *Acad. Sci.*, **110**, 13,672–13,677, http://dx.doi.org/10.1073/ pnas.1305733110.
936 Liu, Z., and M. A. Alexander, 2007: Atmospheric Bridge, Oceanic Tunnel and Global
937 Climatic Teleconnections. *Rev*. *Geophys*., **45**, RG2005, doi:10.1029/2005RG000172.
938 MacDonald, G. M., and R. A. Case, 2005: Variations in the Pacific Decadal Oscillation
939 over the past millennium. *Geophys. Res. Lett*, **32**, L08703, doi:10.1029/2005GL022478.
940 Mantua, N. J., S. R. Hare, Y. Zhang, J. M. Wallace, and R. C. Francis, 1997: A Pacific
941 Interdecadal Climate Oscillation with Impacts on Salmon Production. *Bull. Amer.*
942 *Meteor. Soc*, **78**, 1069–1079.
943 McCabe, G. J., and M. D. Dettinger, 1999: Decadal variations in the strength of ENSO
944 teleconnections with precipitation in the western United States. *Int. J. Climatol*, **19**,
945 1399–1410.
946 McCabe, G. J., and M. D. Dettinger, 2002: Primary Modes and Predictability of Year-to-
947 Year Snowpack Variations in the Western United States from Teleconnections with
948 Pacific Ocean Climate. *J. Hydrometeor*, **3**, 13–25.
949 McCabe, G. J., M. A. Palecki, and J. L. Betancourt, 2004: Pacific and Atlantic Ocean

influences on multidecadal drought frequency in the United States. *Proceedings of the National Academy of Sciences*, **101**, 4136–4141, doi:10.1073/pnas.0306738101.

McCabe, G. J., T. R. Ault, B. I. Cook, J. L. Betancourt, and M. D. Schwartz, 2012: Influences of the El Niño Southern Oscillation and the Pacific Decadal Oscillation on the timing of the North American spring. *Int. J. Climatol*, **32**, 2301–2310, doi:10.1002/joc.3400.

McCabe-Glynn, S., K. R. Johnson, C. Strong, M. Berkelhammer, A. Sinha, H. Cheng, and R. L. Edwards, 2013: Variable North Pacific influence on drought in southwestern North America since AD 854. *Nature Geosci*, **6**, 617–621, doi:10.1038/ngeo1862.

Meehl, G. A., A. Hu, and B. D. Santer, 2009: The Mid-1970s Climate Shift in the Pacific and the Relative Roles of Forced versus Inherent Decadal Variability. *J. Climate*, **22**, 780–792, doi:10.1175/2008JCLI2552.1.

Meehl, G. A., and H. Teng, 2014: CMIP5 multi-model hindcasts for the mid-1970s shift and early 2000s hiatus and predictions for 2016–2035. *Geophys. Res. Lett*, **41**, 1711–1716, doi:10.1002/2014GL059256.

Mehta, V. M., N. J. Rosenberg, and K. Mendoza, 2012: Simulated impacts of three decadal climate variability phenomena on dryland corn and wheat yields in the Missouri River Basin. *Agricultural and Forest Meteorology*, **152**, 109–124, doi:10.1016/j.agrformet.2011.09.011.

Mestas-Nuñez, A. M., and D. B. Enfield, 1999: Rotated global modes of non-ENSO sea surface temperature variability, *J. Clim*., **12**, 2734–2746.

971 Miller, A.J., D.R. Cayan, T.P. Barnett, N.E. Graham, and J.M. Oberhuber, 1994a: The
972 1976-77 climate shift of the Pacific Ocean. *Oceanography* **7**(1), 21–26,
973 http://dx.doi.org/10.5670/oceanog.1994.11.
974 Miller, A. J., D. R. Cayan, T. P. Barnett, N. E. Graham, and J. M. Oberhuber, 1994b:
975 Interdecadal variability of the Pacific Ocean: Model response to observed heat flux and
976 wind stress anomalies. *Climate Dyn.,* **9,** 287–302.
977 Miller, A. J. and N. Schneider, 2000: Interdecadal climate regime dynamics in the North
978 Pacific Ocean: Theories, observations and ecosystem impacts. *Progress in*
979 *Oceanography,* **47**, 355-379.
980 Milotti, E., 1995: Linear processes that produce 1/*f* or flicker noise. *Phys. Rev. E.*, **51**,
981 3087-3103.
982 Minobe, S., 1997: A 50-70 year climatic oscillation over the North Pacific and North
983 America. *Geophys. Res. Lett.*, **24**, pp 683-686.
984 Minobe, S., 2012: Resonance in bidecadal and pentadecadal climate oscillations over the
985 North Pacific: Role in climatic regime shifts. *Geophys. Res. Lett*, **26**, 855–858,
986 doi:10.1029/1999GL900119.
987 Miyasaka, T., and H. Nakamura, 2005: Summertime subtropical highs and tropospheric
988 planetary waves in the Northern Hemisphere. *J. Climate*, **18**, 5046-5065.
989 Mo, K. C., 2010: Interdecadal Modulation of the Impact of ENSO on Precipitation and
990 Temperature over the United States. *J. Climate*, **23**, 3639–3656,
991 doi:10.1175/2010JCLI3553.1.
992 Nakamura, H., G. Lin, T. Yamagata, 1997: Decadal climate variability in the North
993 Pacific during the recent decades. Bull. Amer. Meteor. Soc., 78, 2215-2225.

994 Nakamura, H. and T. Yamagata, 1999: Recent decadal SST variability in the
995 Northwestern Pacific and associated atmospheric anomalies. "Beyond El Niño: Decadal
996 and Interdecadal Climate Variability". A. Navarra ed., Springer, 49-72.
997 Nakamura, H., and A. S, Kazmin, 2003: Decadal changes in the North Pacific oceanic
998 frontal zones as revealed in ship and satellite observations. *J. Geophys. Res.,* 108(C3),
999 3078, doi:10.1029/1999JC000085.
1000 Nakamura, H., T. Sampe, Y. Tanimoto, and A. Shimpo, 2004: Observed associations
1001 among storm tracks, jet streams and midlatitude oceanic fronts, "Earth's Climate: The
1002 Ocean-Atmosphere Interaction", C. Wang, S.-P. Xie and J. A. Carton, Eds., Geophys.
1003 Monogr., **147**, American Geophysical Union, Washington, D.C., U.S.A., 329-346.
1004 Namias, J., and R. M. Born, 1970: Temporal coherence in North Pacific sea-surface
1005 temperature patterns, *J. Geophys. Res*., **75**, 5952 – 5955.
1006 Namias, J., and R. M. Born, 1974: Further studies of temporal coherence in North Pacific
1007 sea surface temperatures. *J. Geophys. Res*., **79**, 797–798.
1008 Newman, M., 2007: Interannual to Decadal Predictability of Tropical and North Pacific
1009 Sea Surface Temperatures. *J. Climate*, **20**, 2333–2356, doi:10.1175/JCLI4165.1.
1010 Newman, M., G. P. Compo, and M. Alexander, 2003: ENSO-Forced Variability of the
1011 Pacific Decadal Oscillation. *J. Climate*, **16**, 3853–3857.
1012 Newman, M., 2013: An empirical benchmark for decadal forecasts of global surface
1013 temperature anomalies. *J. Climate*, **26**, 5260-5269, doi:10.1175/JCLI-D-12-00590.1.
1014 Nonaka, M., H. Nakamura, Y. Tanimoto, T. Kagimoto, and H. Sasaki, 2006: Decadal
1015 Variability in the Kuroshio–Oyashio Extension Simulated in an Eddy-Resolving OGCM.
1016 *J. Climate*, **19**, 1970–1989, doi:10.1175/JCLI3793.1.

1017 Nonaka, M., Sasaki, H., Taguchi, B., & Nakamura, H., 2012: Potential predictability of
1018 interannual variability in the Kuroshio Extension jet speed in an eddy-resolving OGCM.
1019 *J. Climate*, **25**(10), 3645-3652.
1020 Norris, J. R., 1998: Low cloud type over the ocean from surface observations. Part II:
1021 Geographic and seasonal variations. *J. Climate*, **11**, 383–403.
1022 Norris, J. R., Y. Zhang, and J. M. Wallace, 1998: Role of clouds in summertime
1023 atmosphere-ocean interactions over the North Pacific. *J. Clim*., **11**, 2482–2490.
1024 Nurhati, I., K.M. Cobb, and E. Di Lorenzo, 2011: Decadal-scale SST and salinity
1025 variations in the central tropical Pacific: signatures of natural and anthropogenic climate
1026 change. *J. Climate*, doi: 10.1175/2011JCLI3852.1.
1027 O'Reilly, C. H., and A. Czaja, 2015: The response of the Pacific storm track and
1028 atmospheric circulation to Kuroshio Extension variability. *Quart. J. R. Met. Soc*, in press,
1029 doi: 10.1002/qj.2334
1030 Oakley, N. S., and K. T. Redmond, 2014: A Climatology of 500-hPa Closed Lows in the
1031 Northeastern Pacific Ocean, 1948–2011. *J. Appl. Meteor. Climatol.*, **53**, 1578–1592,
1032 doi:10.1175/JAMC-D-13-0223.1.
1033 Okajima, S., H. Nakamura, K. Nishii, T. Miyasaka, and A. Kuwano-Yoshida, 2014:
1034 Assessing the importance of prominent warm SST anomalies over the midlatitude North
1035 Pacific in forcing large-scale atmospheric anomalies during 2011 summer and autumn. *J.*
1036 *Climate*, **27**, 3889–3903, doi:10.1175/JCLI-D-13-00140.1.
1037 Oldenborgh, G.J. van, F.J. Doblas-Reyes, B. Wouters and W. Hazeleger, 2012: Skill in
1038 the trend and internal variability in a multi-model decadal prediction ensemble. *Clim.*
1039 *Dyn.,* **38**, 1263-1280, doi:10.1007/s00382-012-1313-4.

1040 Oshima, K., and Y. Tanimoto, 2009: An evaluation of reproducibility of the Pacific
1041 decadal oscillation in the CMIP3 simulations. *J Meteorol Soc Japan*, **87**(4):755–770.
1042 Overland, J. E., J. Alheit, A. Bakun, J. W. Hurrell, D. L. Mackas, and A. J. Miller, 2010:
1043 Climate controls on marine ecosystems and fish populations. *Journal of Marine Systems*,
1044 **79**, 305–315, doi:10.1016/j.jmarsys.2008.12.009.
1045 Overland, J. E., D. B. Percival, and H. O. Mofjeld, 2006: Regime shifts and red noise in
1046 the North Paciifc. *Deep-Sea Research I*, **53**, 582-588.
1047 Park, J.-H., S. I. An, S.-W. Yeh, and N. Schneider, 2013: Quantitative assessment of the
1048 climate components driving the pacific decadal oscillation in climate models. *Theor Appl*
1049 *Climatol*., **112**, 431–445, doi:10.1007/s00704-012-0730-y.
1050 Parker, D., C. Folland, A. Scaife, J. Knight, A. Colman, P. Baines, and B. Dong, 2007:
1051 Decadal to multidecadal variability and the climate change background. *J. Geophys. Res*.,
1052 **112**, D18115, doi:10.1029/2007JD008411.
1053 Pederson, G. T., S. T. Gray, T. Ault, W. Marsh, D. B. Fagre, A. G. Bunn, C. A.
1054 Woodhouse, and L. J. Graumlich, 2011: Climatic Controls on the Snowmelt Hydrology
1055 of the Northern Rocky Mountains. *J. Climate*, **24**, 1666–1687,
1056 doi:10.1175/2010JCLI3729.1.
1057 Penland, C., and P. D. Sardeshmukh, 1995: The optimal growth of tropical sea surface
1058 temperature anomalies. *J. Climate*, **8**, 1999—2024.
1059 Penland, C., and P. D. Sardeshmukh, 2012: Alternative interpretations of power-law
1060 distributions found in nature. *Chaos*, **22**, 023119, doi:10.1063/1.4706504.
1061 Percival, D. B., J. E. Overland, and H. O. Mofjeld, 2001: Interpretation of North Pacific
1062 variability as a short- and long-memory process. *J. Climate*, **14**, 4545-4559.

1063 Peterson, W.T., and J.E. Keister, 2003: Interannual variability in copepod community
1064 composition at a coastal station in the northern California Current: a multivariate
1065 approach. *Deep-Sea Research Part II: Topical Studies In Oceanography*, **50** (14-16),
1066 2499-2517.
1067 Peterson, W.T., and F. B. Schwing, 2003: A new climate regime in northeast Pacific
1068 ecosystems. *Geophys. Res. Lett.*, **30**, 1896, doi:10.1029/2003GL017528.
1069 Phillips, A. S., C. Deser, and J. Fasullo, 2014: A New Tool for Evaluating Modes of
1070 Variability in Climate Models. *EOS*, **95**, 453-455, doi: 10.1002/2014EO490002.
1071 Pierce, D. W., 2001: Distinguishing coupled ocean–atmosphere interactions from
1072 background noise in the North Pacific. *Progress in Oceanography*, **49**, 331–352,
1073 doi:10.1016/S0079-6611(01)00029-5.
1074 Pierce, D. W., 2002: The Role of Sea Surface Temperatures in Interactions between
1075 ENSO and the North Pacific Oscillation. *J. Climate*, **15**, 1295–1308, doi:10.1175/1520-
1076 0442(2002)015<1295:TROSST>2.0.CO;2.
1077 Polade, S. D., A. Gershunov, D. R. Cayan, M. D. Dettinger, and D. W. Pierce, 2013:
1078 Natural climate variability and teleconnections to precipitation over the Pacific-North
1079 American region in CMIP3 and CMIP5 models. *Geophys. Res. Lett*, **40**, 2296–2301,
1080 doi:10.1002/grl.50491.
1081 Power, S., M. Haylock, R. Colman, and X. Wang, The Predictability of Interdecadal
1082 Changes in ENSO Activity and ENSO Teleconnections. *journals.ametsoc.org*.
1083 Power, S., T. Casey, C. Folland, A. Colman, and V. Mehta, 1999: Inter-decadal
1084 modulation of the impact of ENSO on Australia. *Clim Dyn*, **15**, 319–324,
1085 doi:10.1007/s003820050284.

1086 Qiu, B., 2000: Interannual variability of the Kuroshio extension system and its impact on
1087 the wintertime SST field. *J. Phys. Oceanogr.*, **30**, 1486-1502.
1088 Qiu, B., 2002: The Kuroshio Extension system: Its large-scale variability and role in the
1089 midlatitude ocean-atmosphere interaction. *J. Oceanogr.*, **58**, 57-75.
1090 Qiu, B., 2003: Kuroshio Extension variability and forcing of the Pacific decadal
1091 oscillations: Responses and potential feedback. *J. Phys. Oceanogr*., **33**, 2465–2482.
1092 Qiu, B., and S. Chen, 2005: Variability of the Kuroshio Extension Jet, Recirculation
1093 Gyre, and Mesoscale Eddies on Decadal Time Scales. *J. Phys. Oceanogr.*, **35**, 2090–
1094 2103.
1095 Qiu, B., and S. Chen, 2010: Eddy-mean flow interaction in the decadally-modulating
1096 Kuroshio Extension system. *Deep-Sea Res. II*, **57**, 1098-1110.
1097 Qiu, B., N. Schneider, and S. Chen, 2007: Coupled Decadal Variability in the North
1098 Pacific: An Observationally Constrained Idealized Model. *J. Climate*, **20**, 3602–3620,
1099 doi:10.1175/JCLI4190.1.
1100 Qiu, B., S. Chen, N. Schneider, and B. Taguchi, 2014: A Coupled Decadal Prediction of
1101 the Dynamic State of the Kuroshio Extension System. *J. Climate*, **27**, 1751–1764,
1102 doi:10.1175/JCLI-D-13-00318.1.
1103 Rayner, N. A., D. E. Parker, E. B. Horton, C. K. Folland, L. V. Alexander, D. P. Rowell,
1104 E. C. Kent, and A. Kaplan, 2003: Global analyses of sea surface temperature, sea ice, and
1105 night marine air temperature since the late nineteenth century. *J. Geophy Res*., **108**, 4407,
1106 doi:10.1029/2002JD002670.

1107 Reynolds, R. W., T. M. Smith, C. Liu, D. B. Chelton, K. S. Casey and M. G. Schlax,
1108 2007: Daily high-resolution blended analyses for sea surface temperature, *J. Climate*, **20**,
1109 5473-5496)
1110 Rudnick, D. L., and R. E. Davis, 2003: Red noise and regime shifts. *Deep Sea Research*
1111 *I*, **50**, 691-699.
1112 St George, S., 2014: An overview of tree-ring width records across the Northern
1113 Hemisphere. *Quaternary Science Reviews*, **95**, 132–150,
1114 doi:10.1016/j.quascirev.2014.04.029.
1115 Saravanan, R., and J. C. McWilliams, 1998: Advective ocean-atmosphere interaction: An
1116 analytical stochastic model with implications for decadal variability. *J. Climate*.
1117 Sasaki, Y. N., and N. Schneider, 2011: Decadal shifts of the Kuroshio Extension jet:
1118 Application of thin-jet theory. *J. Phys. Ocean*., **41**, 979-993.
1119 Sasaki, Y. N., S. Minobe and N. Schneider, 2013: Decadal response of the Kuroshio
1120 Extension jet to Rossby waves: Observation and thin-jet theory. *J. Phys. Ocean*, **43**, 442-
1121 456.
1122 Schindler, D.E., L.A. Rogers, 2009: Responses of salmon populations to climate variation
1123 in freshwater ecosystems. Pages 1127-1142 in CG Krueger, CE Zimmerman (eds),
1124 Arctic-Yukon-Kuskokwim Sustainable Salmon Initiative. Am. Fish. Soc. Symp.
1125 Schneider, N., A. J. Miller, and D. W. Pierce, 2002: Anatomy of North Pacific Decadal
1126 Variability. *J. Climate*, **15**, 586–605.
1127 Schneider, N., and A. J. Miller, 2001: Predicting Western North Pacific Ocean Climate.
1128 *J. Climate*, **14**, 3997–4002.
1129 Schneider, N., and B. D. Cornuelle, 2005: The Forcing of the Pacific Decadal Oscillation.

J. Climate, **18**, 4355–4373, doi:10.1175/JCLI3527.1.

Seager, R., A. R. Karspeck, M.A. Cane, Y. Kushnir, A. Giannini, A. Kaplan, B. Kerman, and J. Velez, 2004: Predicting Pacific decadal variability. In *Earth's Climate: The Ocean-Atmosphere Interaction*, Geophysical Monograph Series 147, 105-120.

Seager, R., Y. Kushnir, N. H. Naik, M. A. Cane, and J. Miller, 2001: Wind-Driven Shifts in the Latitude of the Kuroshio–Oyashio Extension and Generation of SST Anomalies on Decadal Timescales. *J. Climate*, **14**, 4249–4265.

Shakun, J. D., and J. Shaman, 2009: Tropical origins of North and South Pacific decadal variability. *Geophys. Res. Lett*, **36**, L19711, doi:10.1029/2009GL040313.

Sheffield, J., and Coauthors, 2013: North American Climate in CMIP5 Experiments. Part II: Evaluation of Historical Simulations of Intraseasonal to Decadal Variability. *J. Climate*, **26**, 9247–9290, doi:10.1175/JCLI-D-12-00593.1.

Shen, C., W.-C. Wang, W. Gong, and Z. Hao, 2006: A Pacific Decadal Oscillation record since 1470 AD reconstructed from proxy data of summer rainfall over eastern China. *Geophys. Res. Lett.*, **33**, L03702, doi:10.1029/2005GL024804.

Smirnov, D., M. Newman, and M. A. Alexander, 2014: Investigating the role of ocean-atmosphere coupling in the North Pacific Ocean. *J. Climate*, **27**, 592-606, doi:10.1175/JCLI-D-13-00123.1.

Smirnov, D., M. Newman, M. A. Alexander, Y.-O. Kwon, and C. Frankignoul, 2015: Investigating the local atmospheric response to a realistic shift in the Oyashio sea surface temperature front. *J. Climate*, **28**, 1126-1147.

1151 Smith, T.M., R.W. Reynolds, T.C. Peterson, and J. Lawrimore, 2008: Improvements to
1152 NOAA's Historical Merged Land–Ocean Temp Analysis (1880–2006). *Journal of*
1153 *Climate*, **21**, 2283–2296.
1154 Stachura, M., N.J. Mantua, and M. Scheuerrell, 2014: Oceanographic influences on
1155 patterns in North Pacific salmon abundance. *Canadian Journal of Fisheries and Aquatic*
1156 *Sciences*, **71**(2): 226-235, 10.1139/cjfas-2013-0367.
1157 Steele, J. H., 2004: Regime shifts in the ocean: reconciling observations and theory.
1158 *Progress in Oceanography*, **60**, 135–141, doi:10.1016/j.pocean.2004.02.004.
1159 Strong, C., and G. Magnusdottir, 2009: The Role of Tropospheric Rossby Wave Breaking
1160 in the Pacific Decadal Oscillation. *J. Climate*, **22**, 1819–1833,
1161 doi:10.1175/2008JCLI2593.1.
1162 Sugimoto S., and K. Hanawa, 2011: Roles of SST anomalies on the wintertime turbulent heat
1163 fluxes in the Kuroshio-Oyashio Confluence Region: influences of warm eddies detached
1164 from the Kuroshio Extension. *J. Climate, **24***, 6551-6561.
1165 Taguchi, B., S.-P. Xie, N. Schneider, M. Nonaka, H. Sasaki, and Y. Sasai, 2007: Decadal
1166 variability of the Kuroshio Extension: Observations and an eddy-resolving model
1167 hindcast. *J. Climate*, **20**, 2357-2377.
1168 Taguchi, B., H. Nakamura, M. Nonaka, N. Komori, A. Kuwano-Yoshida, K. Takaya, and
1169 A. Goto, 2012: Seasonal Evolutions of Atmospheric Response to Decadal SST
1170 Anomalies in the North Pacific Subarctic Frontal Zone: Observations and a Coupled
1171 Model Simulation. *J. Climate*, **25**, 111–139, doi:10.1175/JCLI-D-11-00046.1.
1172 Takasuka, A., Y. Oozeki, H. Kubota, S. E. Lluch-Cota, 2008: Contrasting spawning
1173 temperature optima: Why are anchovy and sardine regime shifts synchronous across the
1174 North Pacific? *Progress In Oceanography*, **77**(2), 225-232.

1175 Tanimoto, Y., H. Nakamura, T. Kagimoto, and S. Yamane, 2003: An active role of
1176 extratropical sea surface temperature anomalies in determining anomalous turbulent heat
1177 fluxes. *J. Geophys. Res*., **108**(C10), 3304, doi:10.1029/2002JC001750
1178 Taylor, K. E., 2001: Summarizing multiple aspects of model performance in a single
1179 diagram. *J. Geophys. Res.,* **106**(D7), 7183–7192.
1180 Timlin, M. S., M. A. Alexander, and C. Deser, 2002: On the reemergence of North
1181 Atlantic SST anomalies. *J. Clim*., **15**, 2707 – 2712.
1182 Tingley, M. P., P. F. Craigmile, M. Haran, B. Li, E. Mannshardt, and B. Rajaratnam,
1183 2012: Piecing together the past: Statistical insights into paleoclimatic reconstructions.
1184 *Quat. Sci. Rev.*, **35**(0), 1–22, doi:10.1016/ j.quascirev.2012.01.012.
1185 Trenberth, K. E., G. W. Branstator, D. Karoly, A. Kumar, N.-C. Lau, and C. Ropelewski,
1186 1998: Progress during TOGA in understanding and modeling global teleconnections
1187 associated with tropical sea surface temperatures. *J. Geophys. Res*., **103**, 14,291 – 14,324.
1188 Vimont, D. J. 2005: The contribution of the interannual ENSO cycle to the spatial pattern
1189 of decadal ENSO-like variability. *J. Climate*, **18**, 2080-2092.
1190 Vose, R. S., and Coauthors, 2014: Improved Historical Temperature and Precipitation
1191 Time Series for U.S. Climate Divisions. *http://dx.doi.org/10.1175/JAMC-D-13-0248.1*,
1192 53, 1232–1251, doi:10.1175/JAMC-D-13-0248.1.
1193 Walker, G.T. and E.W. Bliss, 1932: World Weather V. *Memoirs of the Royal*
1194 *Meteorological Society*, **4**, (36), 53-84.
1195 Wang, S., J. Huang, Y. He, and Y. Guan, 2014: Combined effects of the Pacific Decadal
1196 Oscillation and El Niño-Southern Oscillation on Global Land Dry–Wet Changes.
1197 *Scientific Reports*, **4**, 6651, doi:10.1038/srep06651.

1198 Wen, C., A. Kumar, and Y. Xue, 2014: Factors contributing to uncertainty in Pacific
1199 Decadal Oscillation index. *Geophys. Res. Lett*, **41**, 7980–7986,
1200 doi:10.1002/2014GL061992.
1201 Wen, C., Y. Xue, and A. Kumar, 2012: Seasonal Prediction of North Pacific SSTs and
1202 PDO in the NCEP CFS Hindcasts. *J. Climate*, **25**, 5689–5710, doi:10.1175/JCLI-D-11-
1203 00556.1.
1204 Wittenberg, A.T., A. Rosati, T. L. Delworth, G. A. Vecchi, and F. Zeng, 2014: ENSO
1205 Modulation: Is It Decadally Predictable?. *J. Climate*, **27**, 2667–2681.
1206 Wood, R., 2012: Stratocumulus clouds. *Mon. Wea. Rev.,* **140**, 2373–2423.
1207 Wu, A., W. W. Hsieh, and A. Shabbar, 2005: The Nonlinear Patterns of North American
1208 Winter Temperature and Precipitation Associated with ENSO. *J. Climate*, **18**, 1736–
1209 1752, doi:10.1175/JCLI3372.1.
1210 Wu, L., Z. Liu, R. Gallimore, R. Jacob, D. Lee, and Y. Zhong, 2003: Pacific Decadal
1211 Variability: The Tropical Pacific Mode and the North Pacific Mode. *J. Climate*, **16**,
1212 1101–1120.
1213 Wu, Z., N. E. Huang, J. M. Wallace, B. V. Smoliak, and X. Chen, 2011: On the time-
1214 varying trend in global-mean surface temperature. *Climate Dynamics*,
1215 doi:10.1007/s00382-011-1128-8.
1216 Yasuda I., H. Sugisaki, Y. Watanabe, S. Minobe, and Y. Oozeki, 1999: Interdecadal
1217 variations in Japanese sardine and ocean/climate. *Fish. Oceanogr*., **8**, 18-24.
1218 Yeh, S.-W., and B. P. Kirtman, 2008: The Low-Frequency Relationship of the Tropical–
1219 North Pacific Sea Surface Temperature Teleconnections. *J. Climate*, **21**, 3416–3432,
1220 doi:10.1175/2007JCLI1648.1.

1221 Yeh, S.-W., X. Wang, C. Wang, and B. Dewitte, 2015: On the Relationship between the
1222 North Pacific Climate Variability and the Central Pacific El Niño. *J. Climate*, **28**, 663–
1223 677, doi:10.1175/JCLI-D-14-00137.1.
1224 Yim, B. Y., M. Kwon, H. S. Min, and J.-S. Kug, 2014: Pacific Decadal Oscillation and its
1225 relation to the extratropical atmospheric variation in CMIP5. *Clim Dyn*, 1–20,
1226 doi:10.1007/s00382-014-2349-4.
1227 Yu, B., and F. W. Zwiers, 2007: The impact of combined ENSO and PDO on the PNA
1228 climate: a 1,000-year climate modeling study. *Clim Dyn*, **29**, 837–851,
1229 doi:10.1007/s00382-007-0267-4.
1230 Yu, J.-Y., Y. Zou, S. T. Kim, and T. Lee, 2012: The Changing Impact of El Nino on US
1231 Winter Temperatures. *Geophys. Res. Lett.*, doi:10.1029/2012GL052483
1232 Zhang, X., J. Wang, F. W. Zwiers, and P. Y. Groisman, 2010: The Influence of Large-
1233 Scale Climate Variability on Winter Maximum Daily Precipitation over North America.
1234 *J. Climate*, **23**, 2902–2915, doi:10.1175/2010JCLI3249.1.
1235 Zhang, Y., J. M. Wallace, and D. S. Battisti, 1997: ENSO-like Interdecadal Variability:
1236 1900–93. *J. Climate*, doi:10.1175/1520-0442(1997)010<1004:ELIV>2.0.CO;2.
1237

Table 1. Paleo reconstructions of the PDO used in Fig.5. Paleoclimate reconstructions were all obtained from the NOAA Paleoclimatology program and are publicly available. Each PDO reconstruction targets slightly different aspects of the PDO, and each follows its own conventions for normalization, so all indices are normalized to unit variance over the period 1901-2000.

Reconstruction	Time period	Proxies used	Season Targeted
Biondi et al. 2001	1661-1991	Tree-ring	ONDJFM*
D'Arrigo and Wilson 2006	1565-1988	Tree-Ring	MAM
MacDonald 2005	993-1996	Tree-Ring	Annual (Jan-Dec)
D'Arrigo et al. 2001	1700-1979	Tree-Ring	NDJFM*
Felis et al. 2010	1873-1994	Coral (Porites)	NDJF
Shen et al. 2006	1470-1998	Historical Docs	Annual

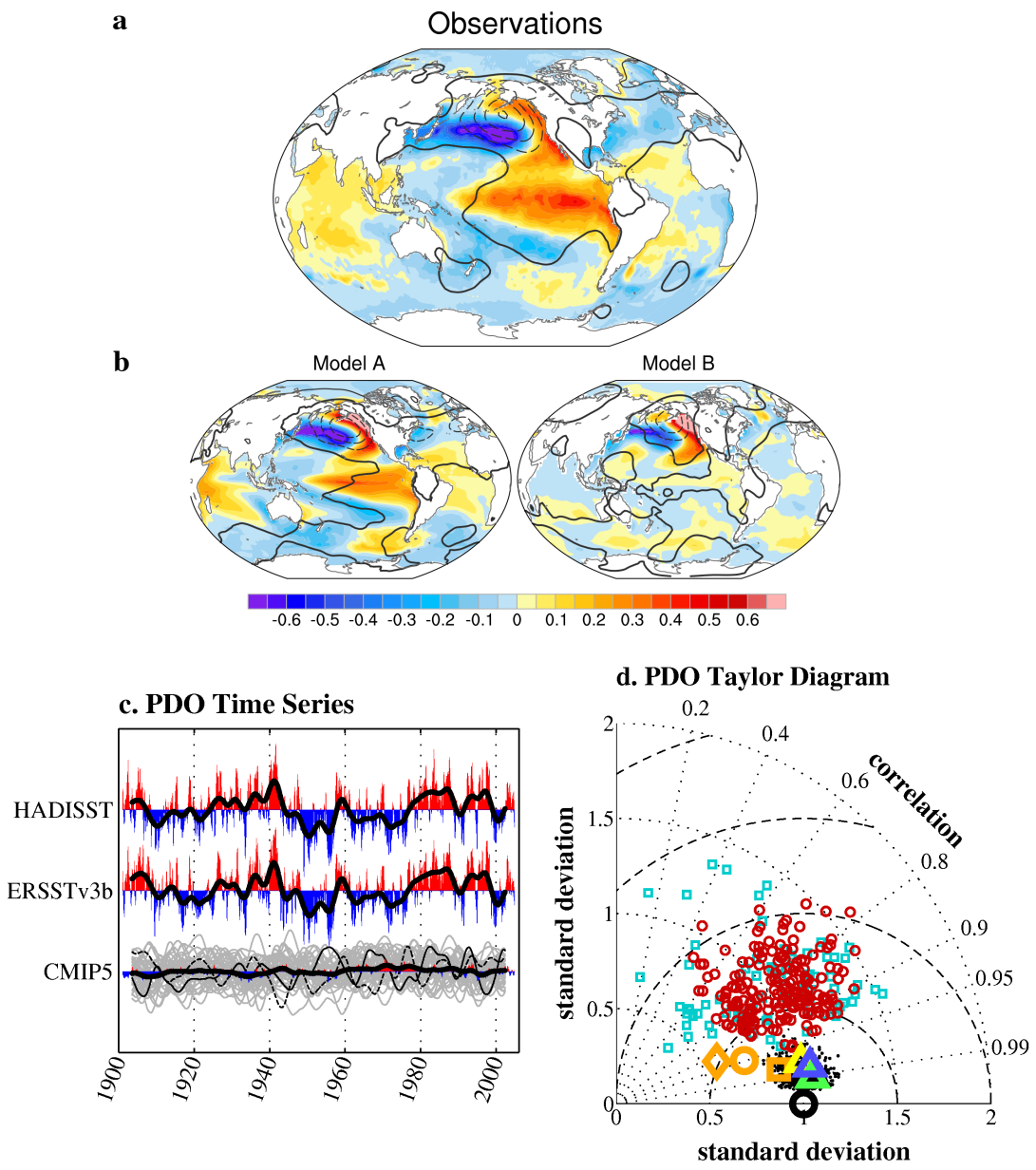

Figure 1. The Pacific decadal oscillation (PDO), in observations and CMIP5 models, over the historical record (1901-2004). (a) Regression of global monthly SST (shading) and DJF SLP (contours; interval is 1 hPa) anomalies onto the PDO time series (from the HadISST dataset). (b) Same as (a) except showing two selected members of the "historical" CMIP5 ensemble. (c) PDO time series determined from the HadISST and ERSST v3b datasets, and from the historical CMIP5 ensemble. For the top two panels, the thick black line shows the smoothed (6-yr lowpass; Zhang et al. 1997) time series. For the last panel, all time series are smoothed; thin gray lines represent each ensemble member, the thin black solid (dashed) line represents model A (B), and the thick black line is the ensemble mean. (d) Taylor diagram (Taylor et al. 2001) comparing the reference PDO (HadISST) pattern (black circle) with variations due to sampling, observational dataset, and geographical domain; the distance of each symbol from the black circle (the reference PDO in Fig. 1a) represents normalized root-mean-square error, indicated by the dashed semicircles spaced at an interval of 0.5. See supplementary material for additional detail. Black dots: PDO estimates based on the 50yr Monte Carlo subsamples; triangles: PDO determined from the ERSSTv3b (blue), COBE (green), and Kaplan (yellow) observed data sets; orange symbols: SSTA structure (within the North Pacific PDO region) associated with the leading SSTA EOF, where the southern border of the Pacific domain is instead 0º (square), 20ºS (triangle), and 70ºS (circle). Also shown are the CMIP3 (cyan squares) and CMIP5 (red circles) historical simulation PDOs.

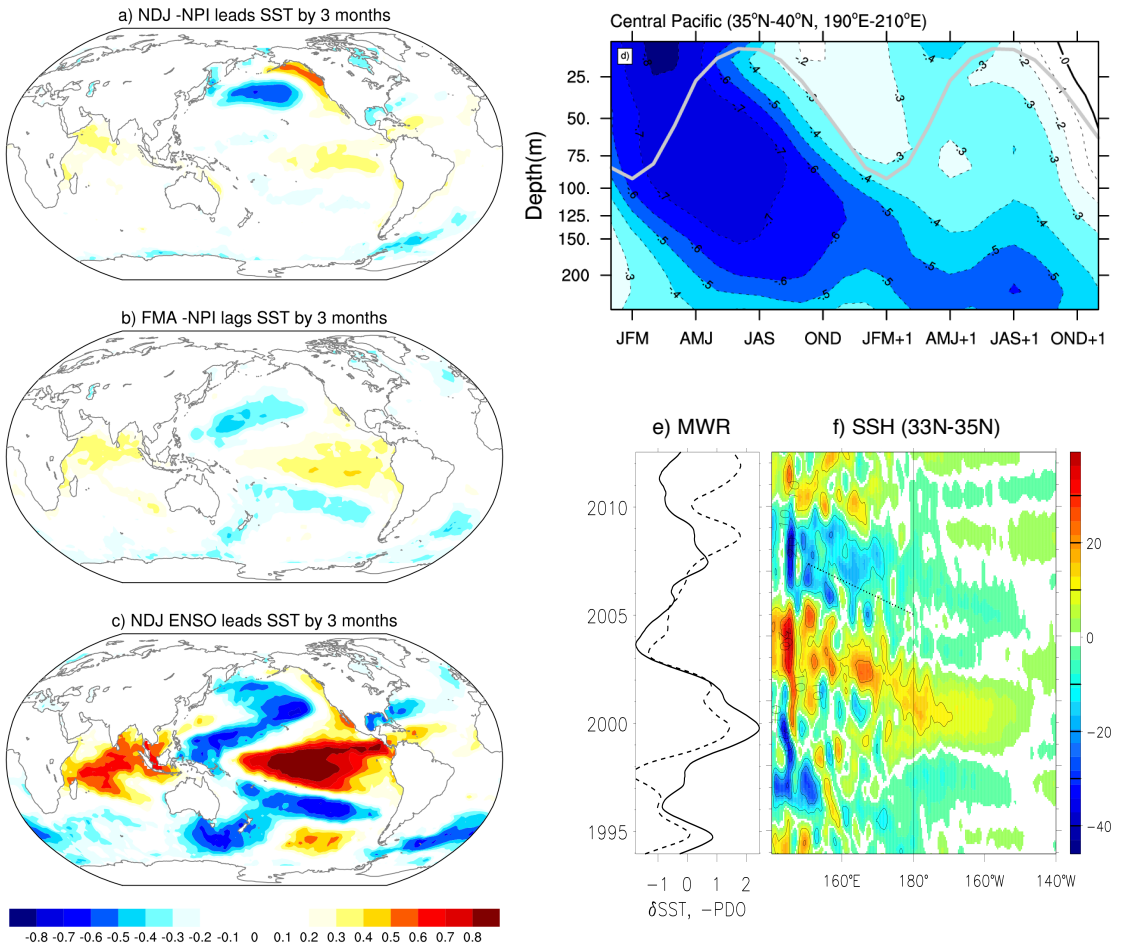

Figure 2. Illustration of "processes" that drive variability of the PDO: local and remote atmospheric forcing (a-c), re-emergence of oceanic thermal anomalies (d), and slow ocean (Rossby wave) dynamics (e-f). (a) One-season lead correlation between DJF NPI and global SSTAs during MMA, 1901-2004. (b) One-season lag correlation between MMA NPI and global SSTAs during DJF, 1901-2004. (c) One-season lag correlation between the DJF value of the "ENSO index" (the leading PC of tropical Pacific SSTA) and global SSTAs during MMA, 1901-2004. In this and subsequent figures, the NPI index sign has been flipped so that "positive" refers to a deepening of the Aleutian low. (d) Correlation of the JFM value of the PDO time series (as in Fig. 1c except determined from 3-month running means) with SODA ocean temperatures (Carton and Giese 2008) area averaged in the Gulf of Alaska, for the years 1958-2004. The gray line shows the climatological mean mixed layer depth as a function of time of year. (e) Time series of the SSTA in the mixed water region (MWR, solid) and the PDO (dashed, with sign inverted). The temperature index is based on the optimal interpolation, blended, quarter degree SST analysis of Reynolds et al. (2007). The MWR extends from the coast of Japan to 150E, and between 36N to 42N. Both the MWR and PDO indices have been normalized by their respective standard deviation. The correlation between MWR and PDO indices is -0.49. (f) Satellite observed sea surface height anomalies in cm, averaged between 33N and 35N. The dotted line marks a westward phase speed of 3.7 cm/s (Qiu and Chen 2010). Sea surface temperature and sea surface height anomalies have been detrended and smoothed with a two year running mean, with weights varying linearly as a function of lag.

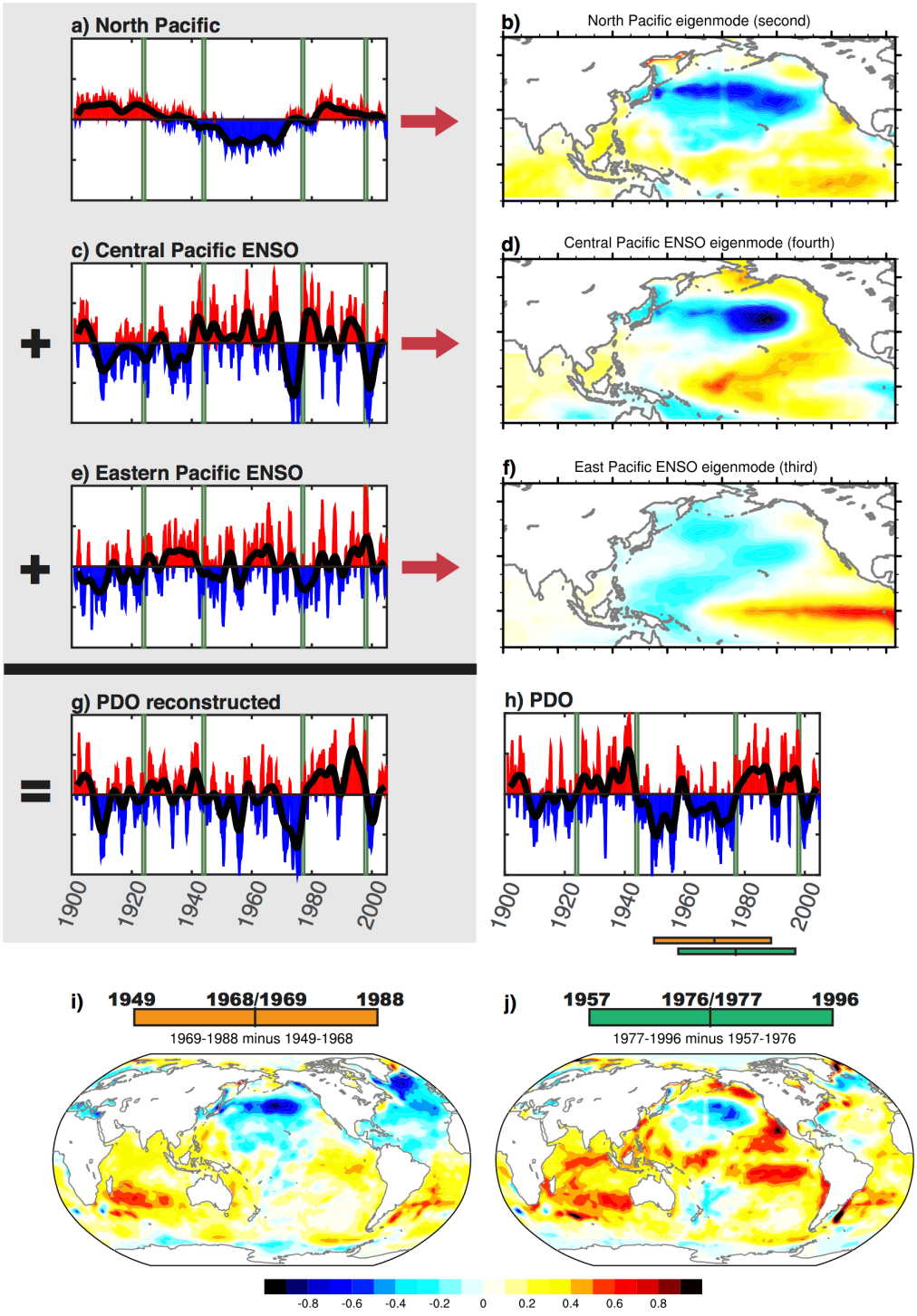

Figure 3. Reconstructing the PDO as the sum of three different processes. (a-h) Contributions to the PDO from (a) the second ("North Pacific"; Fig. 3b), (c) fourth ("Central Pacific ENSO"; Fig. 3d) and (e) third ("Eastern Pacific ENSO"; Fig. 3f shows most energetic phase, with least energetic phase not shown) eigenmodes of the LIM described in the paper. Note that unlike EOFs, these eigenmodes are nonorthogonal. (d) "PDO reconstruction", the sum of the time series shown in panels a, c, and e. (h) PDO time series. In time series panels, heavy black lines represent the application of the same 6-yr lowpass smoother as in Fig. 1c, and green lines indicate times of PDO "regime shifts". (i and j) Epoch difference maps, showing SST differences of two adjacent 20 year means centered on (i) 1968/69 and (j) 1976/77. The adjacent 20-year periods used for each epoch calculation are indicated by the corresponding color bars in Fig. 3h.

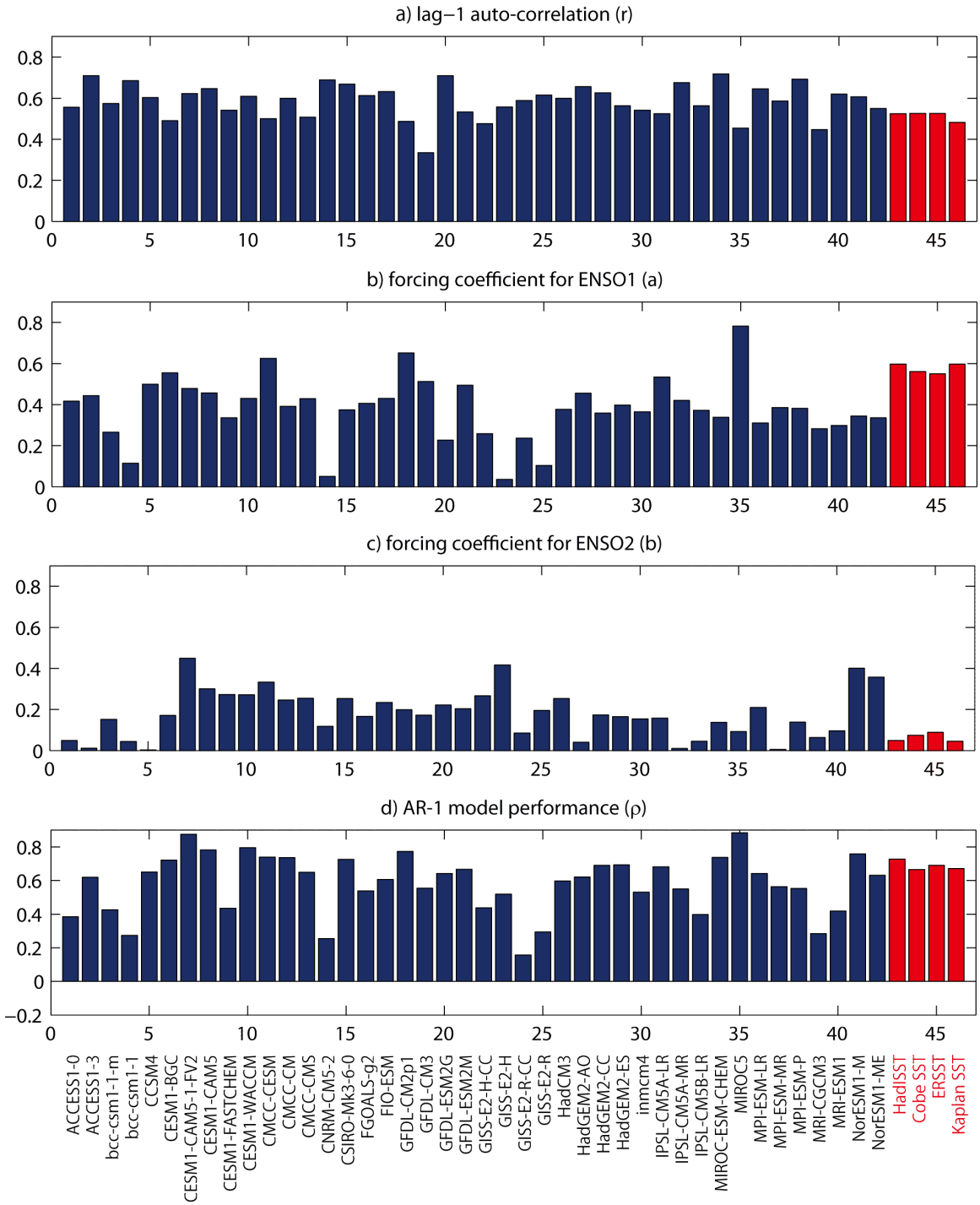

Figure 4. Parameters for an AR-1 model of the PDO time series, PDO(n)=r PDO(n-1) + a ENSO1(n) + b ENSO2(n) + ε, for CMIP5 models (blue bars) and observations (red bars). The AR-1 model is determined from the PDO and two leading tropical PCs, ENSO1 and ENSO2, calculated as discussed earlier but for the period 1900 to 2000, and then averaged from July to June. (a) Lag-1 auto correlation, i.e., r in the above equation. (b) Forcing coefficient for ENSO1, i.e., a in the above equation. (c) Forcing coefficient for ENSO2, i.e., b in the above equation. (d) Correlation ρ between actual PDO time series and estimated PDO timeseries determined from the AR-1 model.

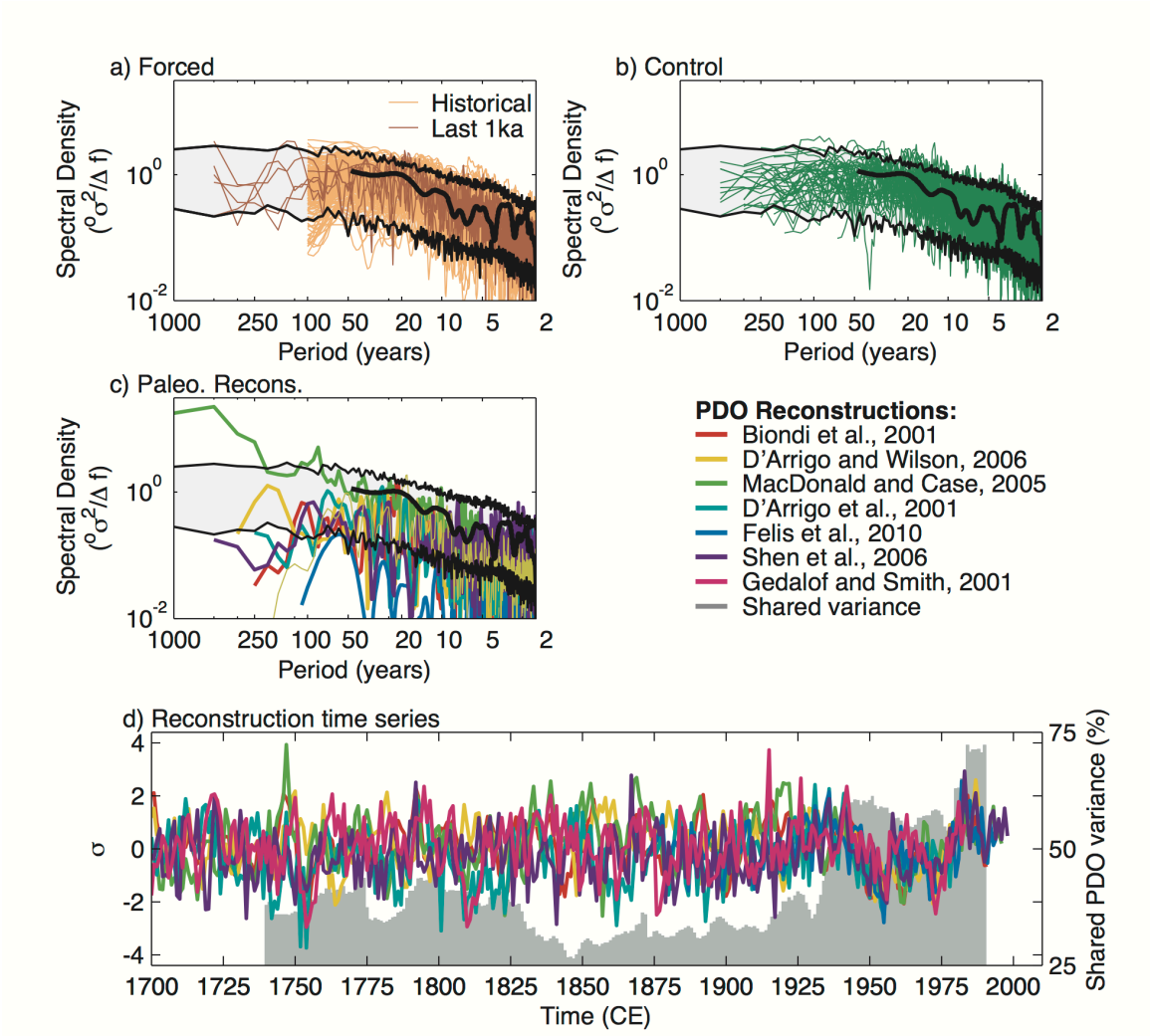

Figure 5. Comparison of observed, paleoclimate, and CMIP5 PDO spectra: (a) CMIP5 "historical" simulations (190 runs total) and forced "last millennium" (past 1000 yrs) simulations (6 runs); (b) unforced "control" simulations (48 runs total); and (c) paleoclimate (tree ring and other proxy-based) reconstructions of the PDO. In each case, only winter (NDJFM) averages are used for consistency between data types. All PDO reconstruction indices were normalized to unit variance over 1901-2000; all other indices were normalized to unit variance overall, not just the reference period. The gray shading and black lines show the upper and lower 95% confidence limits of the PDO power spectrum derived from 140 realizations of a LIM simulation each lasting 1750 years. d) Time series of each PDO reconstruction and the relative similarity of the reconstructions through time. The color lines show the individual reconstructions themselves (left axis), while the gray shading shows the relative similarity (right axis), measured by shared variance of the different indices through time, or the fraction of total variance shared by all reconstructions in the correlation matrix of all time series over a moving 40 year window The ratio is computed by dividing the leading eigenvalue of the reconstruction correlation matrix by the total number of reconstructions available through time.

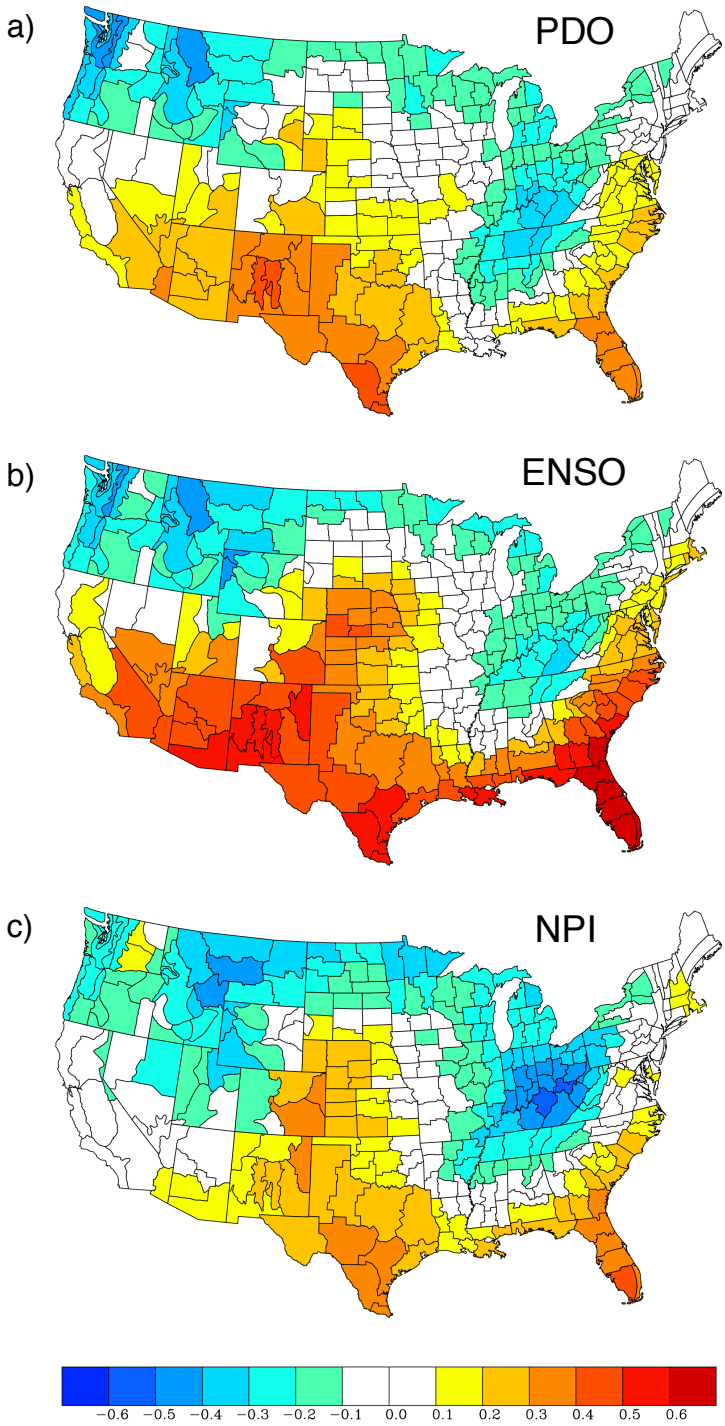

Figure 6. NDJFM US precipitation anomalies (from climate division data; Vose et al. 2014) correlated with (a) the PDO index, (b) the ENSO index, and (c) the NPI, for the years 1901-2004.

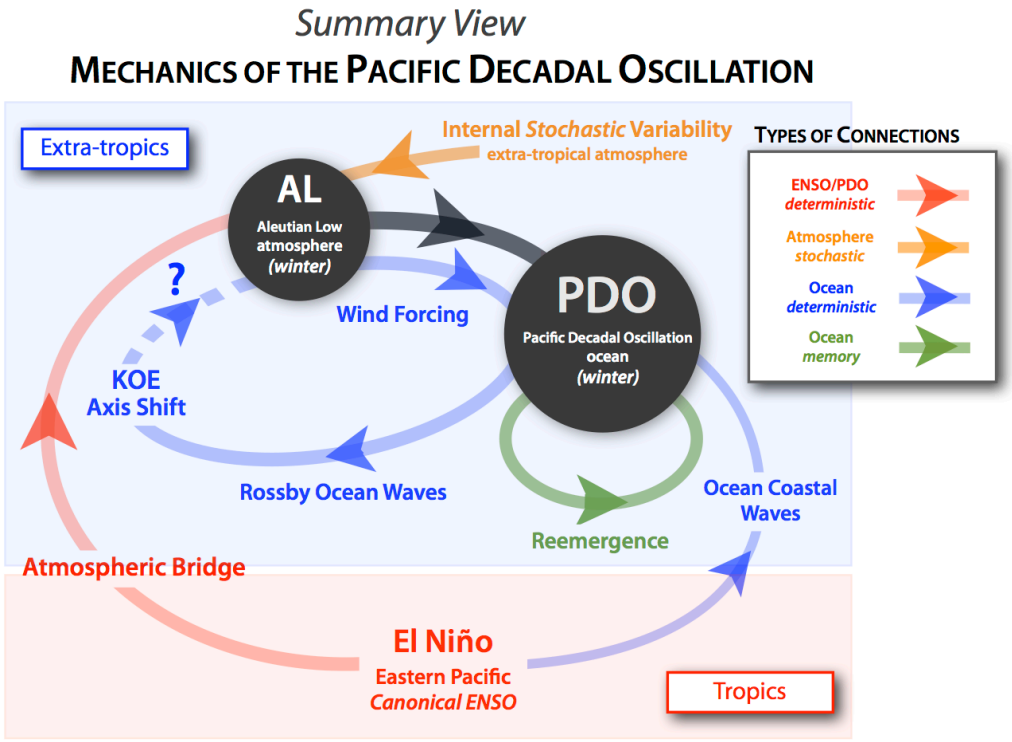

Figure 7. Summary figure of the basic processes involved in the PDO.